Electronic Supplementary Information

Crafting tailored, well-defined block copolymers of cyclic esters with an organomagnesium initiator

Priyanku Nath,[a] Shweta Sagar,[a] Aranya Ray,[a] Himadri Karmakar,[a] Alok Sarkar,[b] Vadapalli Chandrasekhar*[c] and Tarun K. Panda*[a]*

Table of Contents

X-ray crystallographic analysis.

Single crystals of metal complexes **1** were grown from a concentrated solution of toluene/hexane at room temperature. A crystal of suitable dimensions of complexes **1** was mounted on a CryoLoop (Hampton Research Corp.) with a layer of light mineral oil. All the crystals **1** were measured at 293 K. All measurements were made on a Bruker Apex-IV Photon II detector (0.71073 Å) radiation. Crystal data and structure refinement parameters of complexes **1** are summarized in Table TS1. The structures were solved by direct methods (SIR20041 and refined on F2 by full-matrix least-squares methods, using SHELXL-2016/6.2 Non-hydrogen atoms were anisotropically refined. H-atoms were included in the refinement on calculated positions riding on their carrier atoms. The ORTEP-3 program was used to draw the molecules of **1**. The atoms Si1, C14, C15, C28, C29, C30, C31, C32, C33, C44, C45, C46, C47, C48, C49 were found disordered over two positions which have been modelled using standard protocol implemented in SHELXL. Crystallographic data (excluding structure factors) for the structures reported in this paper have been deposited with the Cambridge Crystallographic Data Centre as supplementary publication no. CCDC 2387519 (1). Copies of the data can be obtained free of charge by application to CCDC, 12 Union Road, Cambridge CB21EZ, UK (fax: + (44)1223-336-033; email: deposit@ccdc.cam.ac.uk).

Table TS1. Crystallographic data and refinement parameters of complex **1.**

Crystal parameters	**1**
CCDC NO.	2387519
Empirical formula	$C_{49}H_{69}MgN_4PSi$
Formula weight (g mol^{-1})	797.45
T (K)	293 (2)
λ (Å)	0.71073
Crystal system	Triclinic
Space group	P-1
a (Å)	10.9738(12)
b (Å)	12.7041(12)
c (Å)	18.1148(19)
α (°)	85.417(3)
β (°)	85.746(3)
γ (°)	80.856(3)
V (Å^3)	2480.5(4)
Z	2
D_{calc} (mg m^{-3})	1.068
μ (mm^{-1})	0.127
F(000)	864
θ range for data collection (°)	1.883 to 28.309
Limiting indices	$-14 \leq h \leq 14$, $-16 \leq k \leq 16$, $-24 \leq l \leq 24$
Reflections collected / unique	131794 / 12328 [R_{int} = 0.0978]
Completeness to θ (%)	99.9
Absorption correction	Semi-empirical from equivalents
Max. and min. transmission	1.0000 and 0.8687
Refinement method	Full-matrix least-squares on F^2
Data / restraints / parameters	12328 / 397/ 626
Goodness-of-fit on F^2	1.019
Final R indexes [I>=2σ (I)]	R_1 = 0.0550, wR_2 = 0.1232
Final R indexes (all data)	R_1 = 0.1122, wR_2 = 0.1468

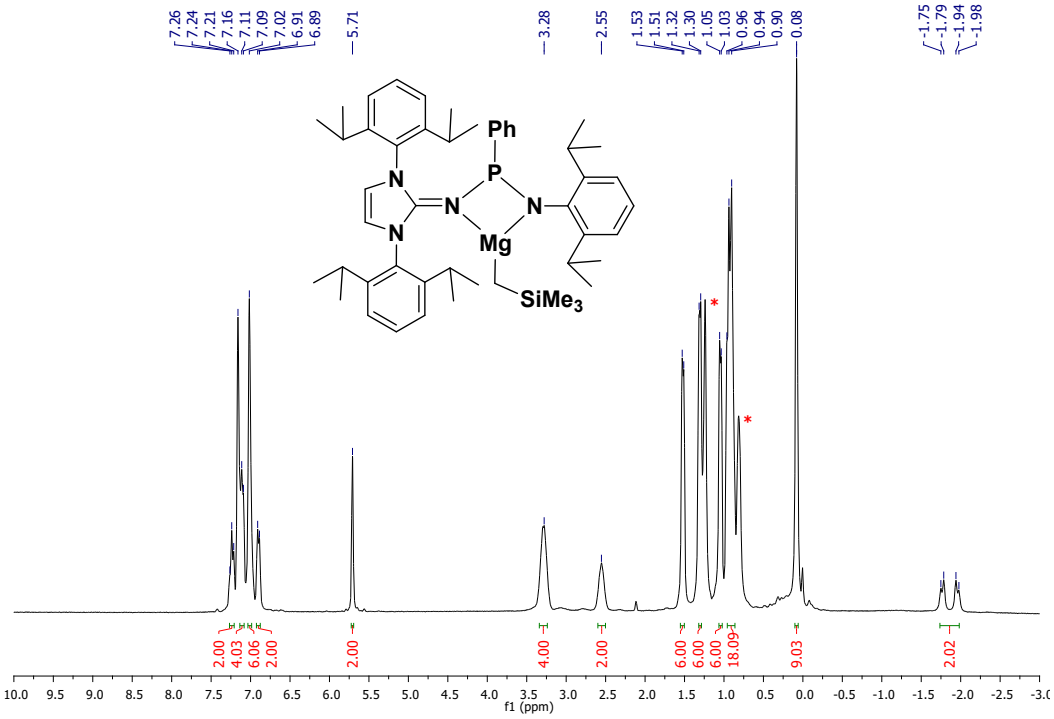

Figure FS1. ^{1}H NMR (300 MHz, C_6D_6, 298 K) spectrum of **1** (**n*-hexane).

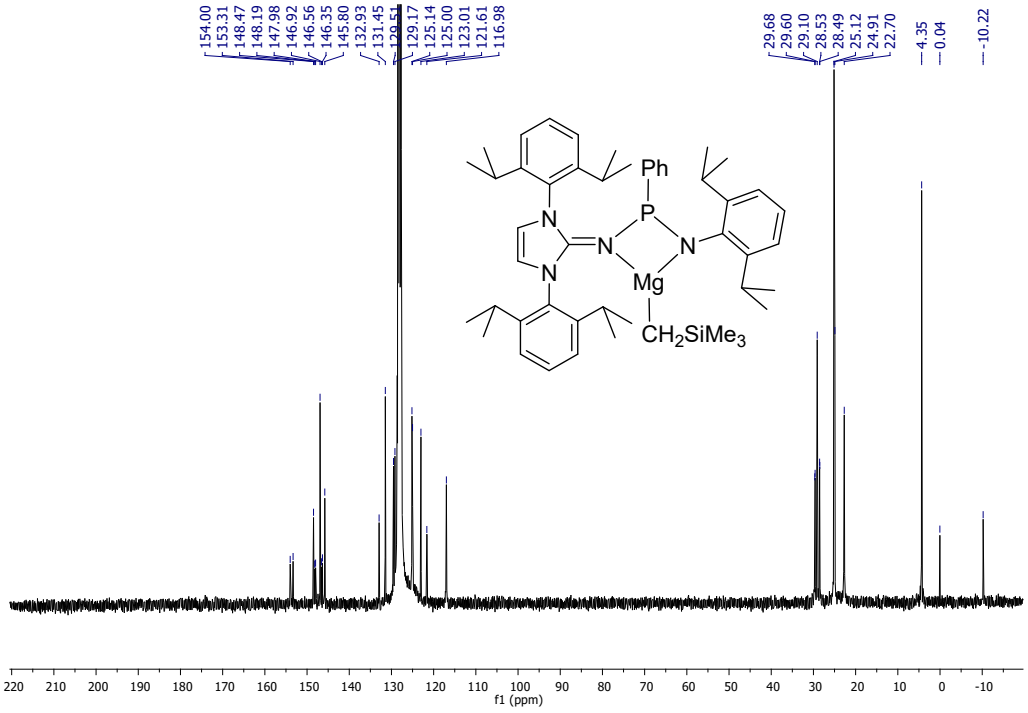

Figure FS2. ^{13}C{^{1}H} NMR (75 MHz, C_6D_6, 298 K) spectrum of **1**.

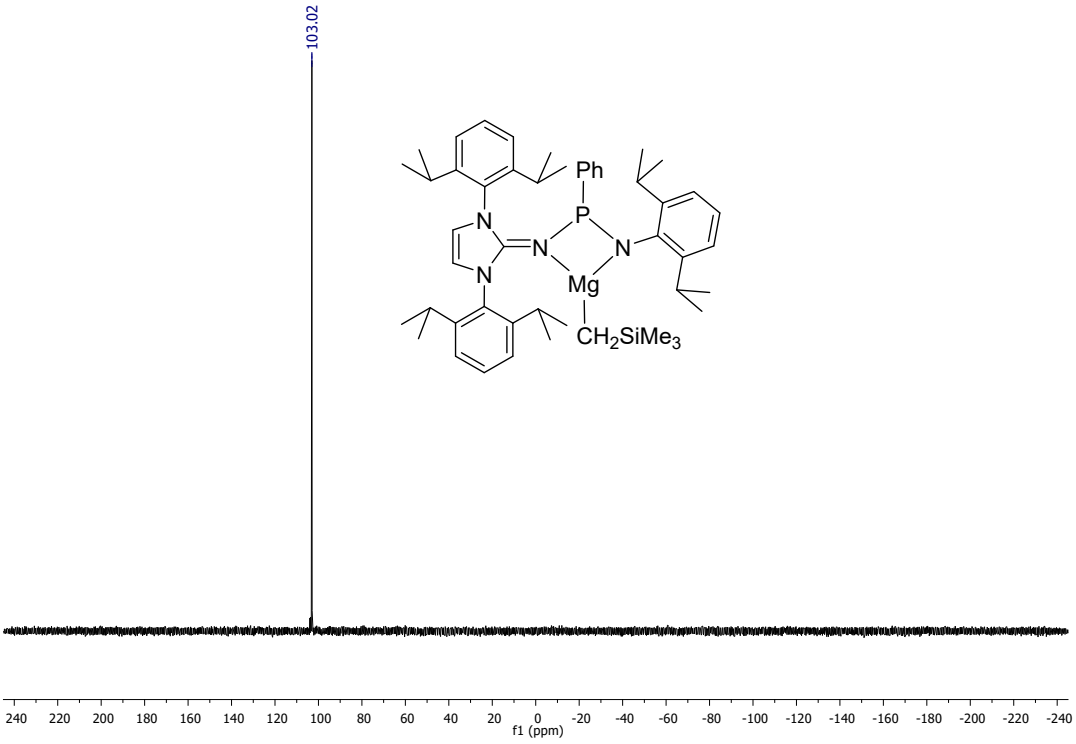

Figure FS3. $^{31}P\{^{1}H\}$ NMR (121.5 MHz, C_6D_6, 298 K) spectrum of **1**.

General

All manipulations involving air- and moisture-sensitive organometallic compounds were carried out under argon using the standard Schlenk technique or argon-filled glove box. Polymerization reactions were carried in dried Schlenk tube equipped with magnetic stirrer. In a typical procedure, first the monomer (ε-CL, *rac*-LA) was added to the solution of catalyst (0.010 g, 0.02 mmol) in toluene (3 ml). Then the solution was stirred at required temperature for a desired reaction time after which the solution was quenched by adding one drop of 2 N HCl and methanol. The solution was concentrated in vacuum and polymer was recrystallized from dichloromethane and hexane followed by methanol precipitation. The final polymer obtained was dried under vacuum to constant weight.

Synthesis of ligand [Im^{Dipp}NP(Ph)NH(Dipp)]

The ligand was prepared by the previously published procedure.[1]

Synthesis of [κ^2-{NHI^{Dipp}P(Ph)NDipp}MgCH$_2$SiMe$_3$] [Dipp = 2,6- diisopropylphenyl] (1)

In an oven-dried 25 ml Schlenk flask, ligand (500 mg, 0.728 mmol) was taken and dissolved in 15 ml of toluene under an argon atmosphere. Then, $Mg(CH_2SiMe_3)_2$ (145 mg, 0.728 mmol) was added to it and stirred at room temperature for 16 h. Next, the solvent was removed in vacuo, and the residue was washed with *n*-hexane. The off-white color crude product was obtained, which was further recrystallized from a toluene/hexane mixture.

1: Yield: 534 mg, 92%. ^{1}H NMR (300 MHz, C_6D_6, 298 K): δ_H 7.24 (t, J = 7.5 Hz, 2H, Ar-*H*), 7.11 (br, 4H, Ar-*H*), 7.02 (br, 6H, Ar-*H*), 6.90 (d, J = 6 Hz, 2H, Ar-*H*), 5.71 (s, 2H, NC*H*), 3.28 (br, 4H, C*H*$(CH_3)_2$), 2.55 (br, 2H, C*H*$(CH_3)_2$), 1.52 (d, J = 6 Hz, 6H, CH(C*H*$_3)_2$), 1.31 (d, J = 6 Hz, 6H, CH(C*H*$_3)_2$), 1.04 (d, J = 6 Hz, 6H, CH(C*H*$_3)_2$), 0.96 (m, 18H, CH(C*H*$_3)_2$), 0.08 (s, 9H, $CH_2Si(CH_3)_3$), -1.86 (dd, J = 57 Hz, 12 Hz, 2H, $CH_2Si(CH_3)_3$) ppm. ^{13}C{^{1}H} NMR (75 MHz, C_6D_6, 298 K): δ_C 154.0 (NHI-*C*=N), 153.3 (Ar*C*-N) 148.5 (d, Ar*C*-N), 148.1 (d, Ar*C*-N), 146.9 (Ar*C*-P), 146.6 (Ar-*C*), 146.3 (Ar-*C*), 145.8 (d, Ar-*C*), 132.9 (Ar-*C*), 131.4 (Ar-*C*), 129.5 (Ar-*C*), 129.2 (Ar-*C*), 125.1 (d, Ar-*C*), 123.0 (Ar-*C*), 121.6 (Ar-*C*), 117.0 (NHI-*C*=*C*), 29.6 (d, *C*H$(CH_3)_2$), 29.1 (d, *C*H$(CH_3)_2$), 28.5 (d, *C*H$(CH_3)_2$), 25.1 (CH(*C*H$_3)_2$), 24.9 (CH(*C*H$_3)_2$), 22.7 (CH(*C*H$_3)_2$), 4.4 ($CH_2Si(CH_3)_3$), -10.2 ($CH_2Si(CH_3)_3$) ppm. ^{31}P{^{1}H} NMR (121.5 MHz, C_6D_6, 298 K): δ_P 103.0 ppm.

Typical polymerization of lactone

First, the monomer (lactone) was added to a solution of the catalyst in toluene. After the solution was reacted at ambient temperature for the desired reaction time, it was quenched with acidified methanol. Then the solution was concentrated in a vacuum and the polymer was recrystallized with dichloromethane and hexane. The final polymer was filtered and dried under vacuum to constant weight.

DSC Analysis

DSC studies were carried out on a SDT Q200 DSC instrument, with a heating rate of 10 ˚C min^{-1} under N_2 flow (50 ml min^{-1}). DSC technical indicators are as follows: maximal sensitivity, 0.2 mw; calorimeter accuracy, prior to 1%; calorimeter precision, prior to 1%; temperature accuracy, < 0.1 ˚C; temperature precision, < 0.01 ˚C. An unsealed Al pan with a 2.0 mg sample was used in the experiments. For ΔH measurements, the DSC system was calibrated with indium (m.p. 156.60 ˚C; ΔH_{fus} = 28.45 J g^{-1}).

TGA analysis

TGA analysis was carried out using a SDT Q600 TGA instrument. TGA technical indicators are as follows: balance sensitivity, 0.1 mg; balance accuracy, prior to 0.1%; balance precision, prior to 0.02%; weighting precision, reach to 10 ppm; temperature precision, ±2 ˚C (measure sample). TGA experiment was carried out under N_2 dynamic atmospheres at a flow rate of 10 ml min^{-1}. 2 mg PCL/PLA sample was heated from 40 to 500 ˚C at 10 ˚C min^{-1} in a nitrogen atmosphere (50 ml min^{-1}).

Details of the Kinetics Study for *rac*–LA Polymerization

A typical kinetics study was conducted to determine the reaction order with respect to the monomer and catalyst. To explore the reaction kinetics, we performed a series of experiments to verify the reaction order. For this, we prepared different concentrations of catalyst **1** (0.005, 0.007, 0.01, 0.015, 0.02 M) in $CDCl_3$ (1 ml) and *rac*-LA (0.072 g, 0.5 mmol) was added at room temperature. The solution was observed for ^{1}H-NMR after heating at ambient temperature for required time intervals. The kinetic plots for $[LA]_0/[LA]$ vs cat **1** were found to be linear, which indicates that there is first-order dependence on *rac*-LA concentration (Figure FS4). Therefore, the rate expression can be summarized as $-d[LA]/dt = k_{app}\,[LA]^1[\kappa^2\text{-}\{NHI^{Dipp}P(Ph)NDipp\}MgCH_2SiMe_3]^x = k_{obs}\,[LA]^1$ where $k_{obs} = k_{app}\,[\kappa^2\text{-}\{NHI^{Dipp}P(Ph)NDipp\}MgCH_2SiMe_3]^x$. Also, a plot of $\ln k_{obs}$ versus $\ln[\kappa^2\text{-}\{NHI^{Dipp}P(Ph)NDipp\}MgCH_2SiMe_3]^x$ is linear indicating the order of $[\kappa^2\text{-}\{NHI^{Dipp}P(Ph)NDipp\}MgCH_2SiMe_3]$ is x = 1.3 (Figure FS6). Since the polymerization reactions showed first order dependence, it substantiates that there is a presence of only one initiator and comprehensively, it's a second-order rate law that can be expressed as

$$\text{rate} = -d[LA]/dt = k_{app}\,[cat]^1\,[LA]^1$$

The activation parameters for the ROP or *rac*-LA in $CDCl_3$ were found to be $\Delta H^{\ddagger}$= 20.197 kJ/mol and $\Delta S^{\ddagger}$= -238.56 J/(mol K), $\Delta Ea^{\ddagger}$ = 23.208 $kJmol^{-1}$. These values were calculated from the temperature-dependent second-order rate constants determined from k_{obs} divided by [**1**] values as provided in (Table TS6) and from the Eyring plot as well as the Arrhenius plot in (Figures 7 and 8). The Eyring plot indicates a similar ordered transition state in a coordination insertion mechanism reported in the literature. A $\Delta G^{\ddagger}$ value of 106.795 kJ/mol was calculated for the ring-opening polymerization of *rac*-LA catalyzed by the catalyst (**1**) at 90 °C.

Table TS2. *rac*-LA polymerizations with time in $CDCl_3$ (1 ml) with different concentrations of catalyst **[1].**

S. No	[LA]/[Cat]	Time (min)	Conversion[a] %	[PLA]	[*rac*-LA]$_t$	[LA]$_0$/[LA]	ln ([LA]$_0$/[LA])
1	100/1	0	0	0	1	1	0
2	100/1	60	5	0.05	0.95	1.05	0.05
3	100/1	120	8	0.08	0.92	1.09	0.08
4	100/1	180	11	0.11	0.89	1.12	0.12
5	100/1	240	17.5	0.175	0.825	1.21	0.19
6	100/1	300	24	0.24	0.76	1.32	0.27
7	100/1	360	31	0.31	0.69	1.45	0.37
8	100/1.5	0	0	0	1	1	0
9	100/1.5	60	11	0.11	0.89	1.12	0.12
10	100/1.5	120	27	0.27	0.73	1.37	0.31
11	100/1.5	180	32	0.32	0.68	1.47	0.39
12	100/1.5	240	45	0.45	0.55	1.81	0.59
13	100/1.5	300	49	0.49	0.51	1.96	0.67
14	100/1.5	360	55	0.55	0.45	2.22	0.79
15	100/2.0	0	0	0	1	1	0
16	100/2.0	60	26.3	0.26	0.74	1.36	0.31
17	100/2.0	120	42.2	0.42	0.58	1.73	0.55
18	100/2.0	180	48.1	0.48	0.52	1.93	0.66
19	100/2.0	240	55.2	0.55	0.45	2.23	0.80
20	100/2.0	300	60	0.6	0.4	2.5	0.92
21	100/2.0	360	67	0.67	0.33	3.03	1.11
22	100/3	0	0	0	1	1	0
23	100/3	60	37.3	0.37	0.63	1.59	0.47
24	100/3	120	49.3	0.49	0.51	1.97	0.68
25	100/3	180	57.5	0.57	0.43	2.35	0.86
26	100/3	240	64.5	0.65	0.36	2.82	1.04
27	100/3	300	72.1	0.72	0.28	3.58	1.28

28	100/3	360	78.3	0.78	0.22	4.61	1.53
29	100/4	0	0	0	1	1	0
30	100/4	60	44.6	0.45	0.55	1.81	0.59
31	100/4	120	65.5	0.66	0.35	2.89	1.06
32	100/4	180	75.2	0.75	0.25	4.03	1.39
33	100/4	240	82	0.82	0.18	5.56	1.71
34	100/4	300	87	0.87	0.13	7.69	2.04
35	100/4	360	93	0.93	0.07	14.29	2.66

[a]Conversion determined through ^{1}H-NMR spectroscopy, [*rac*-LA]$_0$ is taken 1 for calculation. [PLA]$_0$ is zero at t=0.

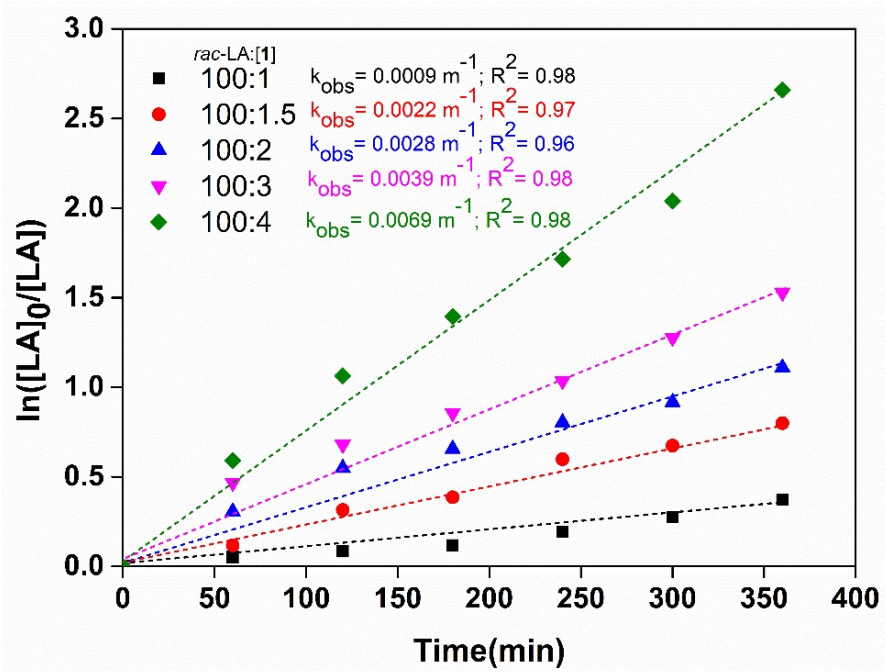

Figure FS4. First-order kinetics plots for *rac*-LA polymerizations (with time) in $CDCl_3$ (1 ml) with different concentrations of complex **1** at 90 °C.

Table TS3. Kinetics plots of k_{obs} vs cat (**1**) for the polymerization of *rac*-LA with [LA] = 0.5 M in $CDCl_3$ (1 ml) at 90 °C.

S. No.	[1] (M)	k_{obs} (m^{-1})
1	0.005	0.0009
2	0.007	0.0022
3	0.01	0.0028

4	0.015	0.0039
5	0.02	0.0069

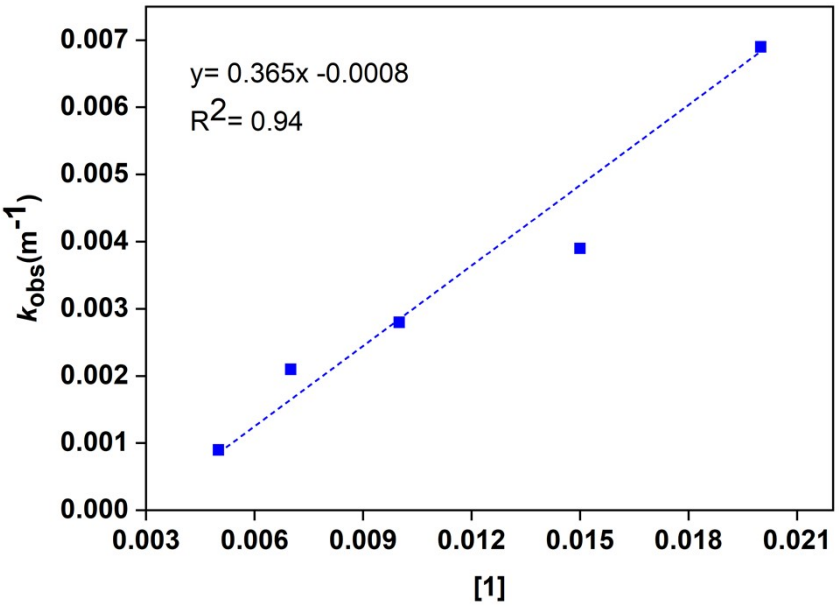

Figure FS5. Kinetics plots of k_{obs} versus in [κ²-{NHI^{Dipp}P(Ph)NDipp}MgCH$_2$SiMe$_3$] for the polymerization of *rac*-LA with [LA] = 0.5 M in $CDCl_3$ (1 ml) at 90 °C.

Table TS4. Kinetics plots of ln k_{obs} vs ln(**1**) for the polymerization of *rac*-LA with [LA] = 0.5 M in $CDCl_3$ (1 ml) at 90 °C.

S. No.	**ln [1]**	**ln k_{obs}**
1	-5.29	-7.01
2	-4.96	-6.12
3	-4.61	-5.88
4	-4.19	-5.55
5	-3.91	-4.98

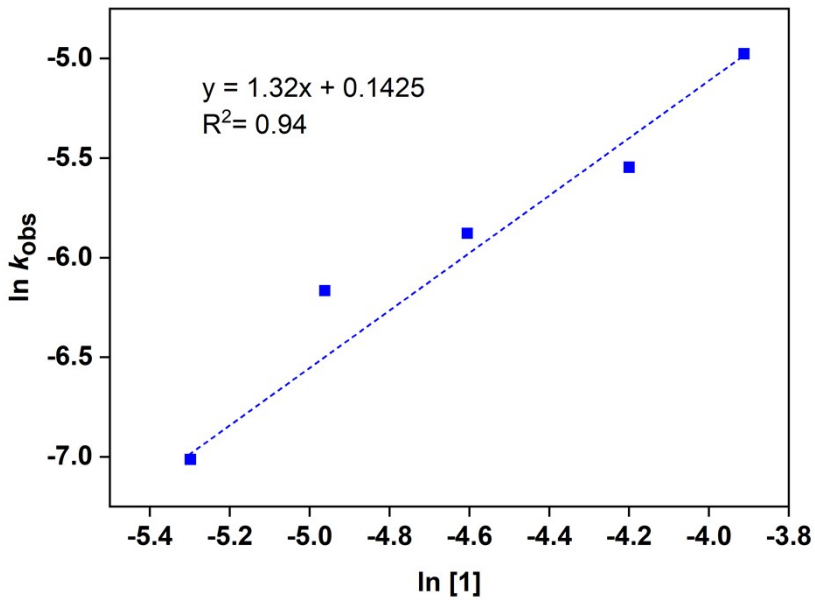

Figure FS6. Kinetics plots of ln k_{obs} versus in ln[κ^2-{NHI^{Dipp}P(Ph)NDipp}MgCH$_2$SiMe$_3$] for the polymerization of *rac*-LA with [LA] = 0.5 M in $CDCl_3$ (1 ml) at 90 ^oC.

Rate of the reaction = $-d[LA]/dt = (0.18)\,[LA]^1[\kappa^2\text{-}\{NHI^{Dipp}P(Ph)NDipp\}MgCH_2SiMe_3]^1$

Eyring Equation:

$$\ln \frac{k}{T} = \frac{-\Delta H^{\ddagger}}{R} \cdot \frac{1}{T} + \ln \frac{k_B}{h} + \frac{-\Delta S^{\ddagger}}{R}$$

Arrhenius Equation:

$$\ln k = \frac{-E_a}{R}\left(\frac{1}{T}\right) + \ln A$$

Where,

- k_B is the Boltzmann's constant (1.381 x 10^{-23} J/K)
- T is the absolute temperature in Kelvin (K)
- h is Planck's constant (6.626 x 10^{-34} Js)
- $\Delta H^{\ddagger}$ is enthalpy of activation (J/(mol K)
- $\Delta S^{\ddagger}$ is entropy of activation (J/(mol K)
- $\Delta E_a^{\ddagger}$ is activation energy (J/(mol K)
- $\Delta G^{\ddagger}$ is Gibbs energy of activation (J/mol)
- R is Gas constant (8.314 J/K mol)

First-order kinetics plots for *rac*- LA polymerizations with time in $CDCl_3$ (1 ml) with different ranges of temperatures catalyzed by **1** is shown in Figure FS7. The activation parameters for the ROP or *rac*-LA in $CDCl_3$ were found to be $\Delta H^{\ddagger}$= 20.197 kJ/mol and $\Delta S^{\ddagger}$= -238.56 J/(mol K), $\Delta Ea^{\ddagger}$ = 23.208 $kJmol^{-1}$. These values were calculated from the temperature-dependent second-order rate constants determined from k_{obs} divided by **[1]** values as provided in (Table TS6) and from the Eyring plot as well as the Arrhenius plot in (Figures FS8 and FS9). The Eyring plot (Figure FS8) indicates a similar ordered transition state in a coordination insertion mechanism reported in the literature. A $\Delta G^{\ddagger}$ value of 106.795 kJ/mol was calculated for the ring-opening polymerization of *rac*-LA catalyzed by the catalyst **(1)** at 90 °C.

Table TS5. *rac*-LA polymerizations with time in $CDCl_3$ (1 ml) at different temperatures of catalyst **[1].** (*rac*-LA:1= 100:2)

S. No	T (K)	Time (min)	Conversion %	[PLA]	$[rac\text{-}LA]_t$	$[LA]_0/[LA]$	$\ln([LA]_0/[LA])$
1	343	0	0	0	1	1	0
2	343	60	16.1	0.16	0.84	1.19	0.18
3	343	120	27.5	0.28	0.73	1.38	0.32
4	343	180	35.4	0.35	0.65	1.55	0.44
5	343	240	41.8	0.42	0.58	1.72	0.54
6	343	300	49.3	0.49	0.51	1.97	0.68
7	343	360	56.1	0.56	0.44	2.28	0.82
8	353	0	0	0	1	1	0
9	353	60	21.5	0.22	0.79	1.27	0.24
10	353	120	37.5	0.38	0.63	1.6	0.47
11	353	180	41.8	0.42	0.58	1.72	0.54
12	353	240	49.7	0.49	0.50	1.99	0.69
13	353	300	55.2	0.55	0.45	2.23	0.80
14	353	360	63.1	0.63	0.37	2.71	0.99
15	363	0	0	0	1	1	0
16	363	60	26.3	0.26	0.74	1.36	0.30
17	363	120	42.2	0.42	0.58	1.73	0.55

18	363	180	48.1	0.48	0.52	1.93	0.66
19	363	240	55.2	0.55	0.45	2.23	0.80
20	363	300	60	0.6	0.4	2.5	0.92
21	363	360	67	0.67	0.33	3.03	1.11
22	373	0	0	0	1	1	0
23	373	60	34.9	0.35	0.65	1.54	0.43
24	373	120	49.2	0.49	0.51	1.97	0.68
25	373	180	55.3	0.55	0.45	2.24	0.81
26	373	240	64.1	0.64	0.36	2.79	1.02
27	373	300	69.5	0.69	0.31	3.28	1.19
28	373	360	79.2	0.79	0.21	4.81	1.57
29	383	0	0	0	1	1	0
30	383	60	38.8	0.39	0.61	1.63	0.49
31	383	120	54.3	0.54	0.46	2.19	0.78
32	383	180	62.5	0.63	0.38	2.67	0.98
33	383	240	73.3	0.73	0.27	3.75	1.32
34	383	300	81.2	0.81	0.19	5.32	1.67
35	383	360	86.1	0.86	0.14	7.19	1.97

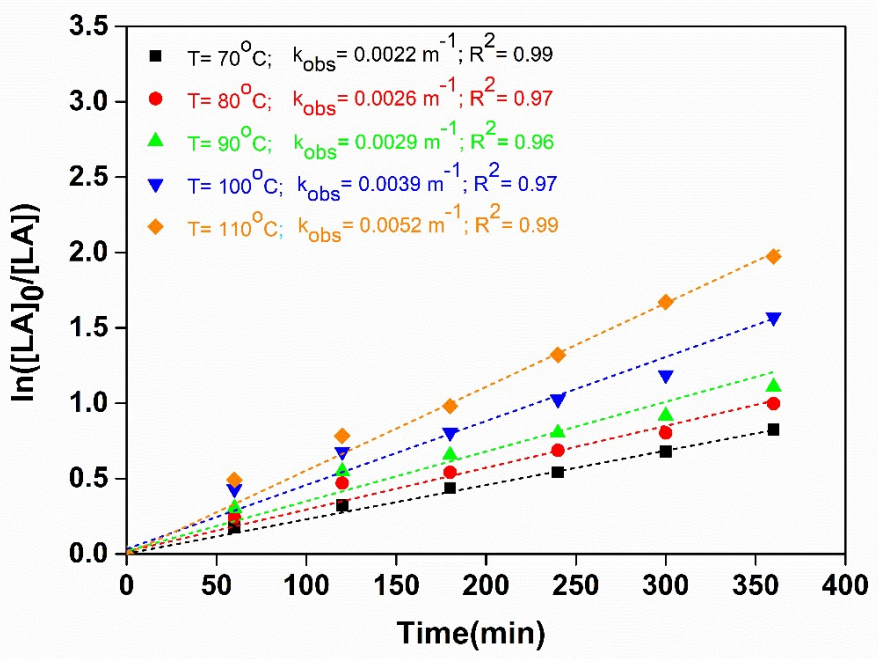

Figure FS7. First-order kinetics plots for *rac* LA polymerizations with time in $CDCl_3$ (1 ml) with different temperatures.

Table TS6. Table for Eyring plot and Arrhenius plot of ln(k_{obs}/T) vs (1/T) catalyzed by [κ^2-{NHI^{Dipp}P(Ph)NDipp}MgCH$_2$SiMe$_3$] (**1**) as a catalyst for the polymerization of *rac*-LA with [LA] = 0.5 M in $CDCl_3$ (1 ml).

Entry	k_{obs}	1/T	ln k_{obs}/T
1	0.0022	0.0030	-11.9
2	0.0026	0.0028	-11.8
3	0.0029	0.0028	-11.74
4	0.0039	0.0027	-11.47
5	0.0052	0.0026	-11.21

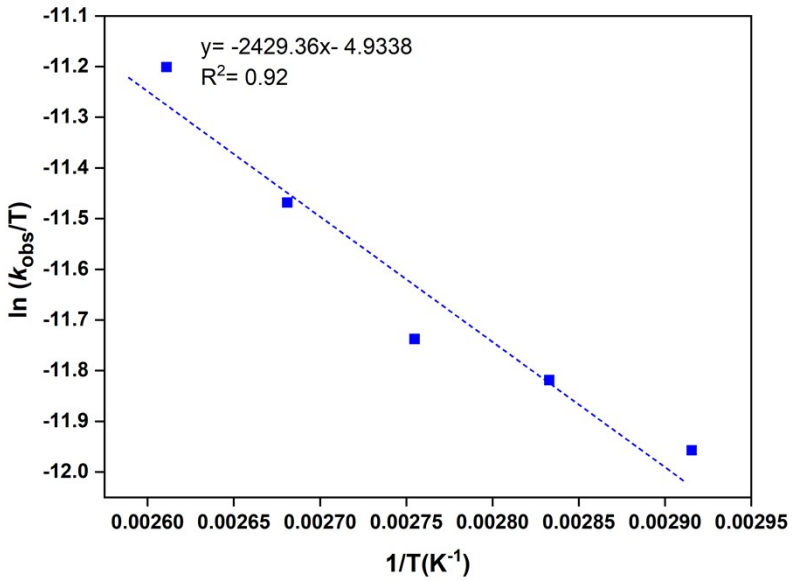

Figure FS8. Eyring plot of ln(k_{obs} /T) ($Mm^{-1}K^{-1}$) vs (1/T) (K^{-1}) for (**1**) cat for the polymerization of *rac*-LA with [LA] = 0.5 M in $CDCl_3$ (1 ml), $\Delta H^{\ddagger}$ = 20.197 kJ mol^{-1} $\Delta S^{\ddagger}$ = -238.56 J mol^{-1}K^{-1} .

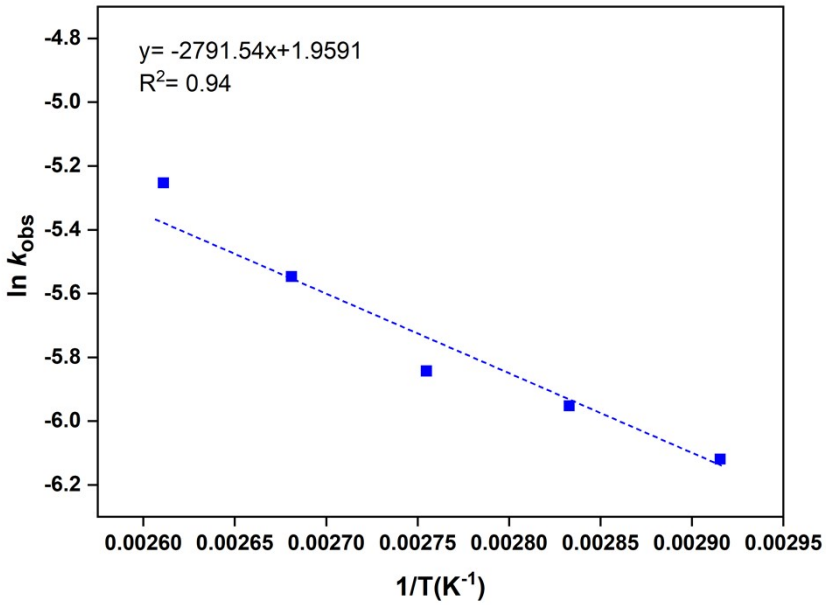

Figure FS9. Arrhenius plots of ln(k_{obs}) (Mm^{-1}) vs (1/T) (K^{-1}) for (**1**) catalyst for the polymerization of *rac*-LA with [LA] = 0.5 M in $CDCl_3$ (1 ml), E_a = 23.208 $kJmol^{-1}$.

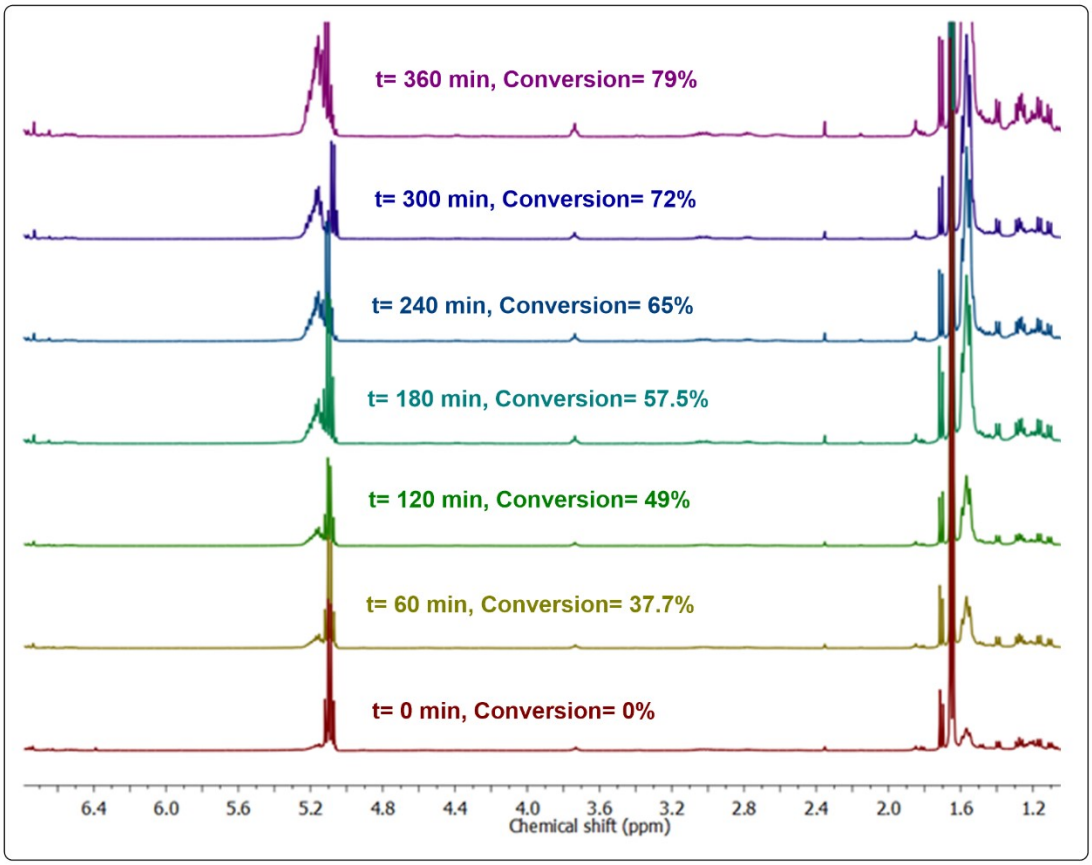

Figure FS10. Stack of ^1H NMR spectra for the kinetic study of the polymerization of [M]:[**1**] = 100:3 of *rac*-LA using **1**. Conditions: [*rac*-LA] = 0.5 M, $CDCl_3$, 90 °C.

Kinetics study in presence of benzyl alcohol as an external initiator

[κ^2-{NHI^{Dipp}P(Ph)NDipp}MgCH$_2$SiMe$_3$]/(1) as a catalyst in the presence of BnOH: A typical kinetics study was performed to establish the reaction order with respect to monomer *rac*–LA, [κ^2-{NHI^{Dipp}P(Ph)NDipp}MgCH$_2$SiMe$_3$] (**1**) and benzyl alcohol. For LA polymerization, *rac*–LA (0.072 g, 0.5 mmol) and benzyl alcohol (0.005 mmol) were added to a solution of **1** (0.005, 0.007, 0.01, 0.015, 0.02 M) in $CDCl_3$ (1 ml), respectively. The solution was set in the NMR tube at 90 °C. After that at the indicated time intervals, the tube was analyzed by ^{1}H NMR spectroscopy. The *rac*-LA concentration [LA] was determined by integrating the quartet methine peak of LA at 5.01 ppm and the broad singlet methine peak at 5.09-5.20 ppm. As expected, plots of $[LA]_0/[LA]$ vs time for a wide range of **1** are linear, indicating the usual first-order dependence on monomer concentration (Figure FS11). Thus, the rate expression can be written as

$$-d[LA]/dt = k_{app}[La]^1[\kappa^2\text{-}\{NHI^{Dipp}P(Ph)NDipp\}MgCH_2SiMe_3]^x = k_{obs}[LA]^1$$

$$\text{where } k_{obs} = k_{app}\,[\kappa^2\text{-}\{NHI^{Dipp}P(Ph)NDipp\}Mg\,CH_2SiMe_3]^x$$

A plot of $\ln(k_{obs})$ vs. $\ln[\kappa^2\text{-}\{NHI^{Dipp}P(Ph)NDipp\}MgCH_2SiMe_3]^x$ (Figure FS11, Table TS7) is linear, indicating the order of $[\kappa^2\text{-}\{NHI^{Dipp}P(Ph)NDipp\}MgCH_2SiMe_3]$ is (x = 1.2 or 1). From the kinetics data, it can be demonstrated that there was almost no change in values for the rate constant for the ROP of *rac*-LA catalyzed by **1** in the presence of benzyl alcohol (Figure FS15).

Table TS7. *rac*-LA polymerizations with time in $CDCl_3$ (1 ml) with different concentrations of catalyst **1 (M)** in the presence of BnOH.

S. No	[LA]/[2]/ BnOH	Time (min)	Conversion %	[PLA]	[rac-LA]$_t$	[LA]$_0$/ [LA]	ln ([LA]$_0$/[LA])
1	100/1.0/1	0	0	0	1	1	0
2	100/1.0/1	60	7	0.07	0.93	1.08	0.07
3	100/1.0/1	120	11	0.11	0.89	1.12	0.12
4	100/1.0/1	180	15	0.15	0.85	1.18	0.16
5	100/1.0/1	240	19.5	0.195	0.805	1.24	0.22
6	100/1.0/1	300	27	0.27	0.73	1.37	0.32
7	100/1.0/1	360	33	0.33	0.67	1.49	0.40
8	100/1.5/1	0	0	0	1	1	0

9	100/1.5/1	60	13	0.13	0.87	1.15	0.14
10	100/1.5/1	120	21	0.21	0.79	1.27	0.24
11	100/1.5/1	180	29	0.29	0.71	1.41	0.34
12	100/1.5/1	240	34	0.34	0.66	1.52	0.42
13	100/1.5/1	300	39	0.39	0.61	1.64	0.49
14	100/1.5/1	360	45	0.45	0.55	1.82	0.59
15	100/2.0/1	0	0	0	1	1	0
16	100/2.0/1	60	20.1	0.201	0.799	1.25	0.22
17	100/2.0/1	120	27.5	0.275	0.725	1.36	0.32
18	100/2.0/1	180	35.7	0.357	0.643	1.56	0.44
19	100/2.0/1	240	41.2	0.412	0.588	1.70	0.53
20	100/2.0/1	300	49.4	0.494	0.506	1.98	0.68
21	100/2.0/1	360	53.8	0.538	0.462	2.16	0.77
22	100/3.0/1	0	0	0	1	1	0
23	100/3.0/1	60	31.3	0.313	0.687	1.46	0.38
24	100/3.0/1	120	39.3	0.393	0.607	1.65	0.49
25	100/3.0/1	180	45.5	0.455	0.545	1.84	0.61
26	100/3.0/1	240	52.5	0.525	0.475	2.11	0.74
27	100/3.0/1	300	61.1	0.611	0.389	2.57	0.94
28	100/3.0/1	360	69.4	0.694	0.306	3.27	1.18
29	100/4.0/1	0	0	0	1	1	0
30	100/4.0/1	60	41.6	0.416	0.584	1.71	0.54
31	100/4.0/1	120	54.5	0.545	0.455	2.19	0.79
32	100/4.0/1	180	71.2	0.712	0.288	3.47	1.25
33	100/4.0/1	240	79	0.79	0.21	4.76	1.56
34	100/4.0/1	300	86	0.86	0.14	7.14	1.97
35	100/4.0/1	360	91	0.91	0.09	11.11	2.41

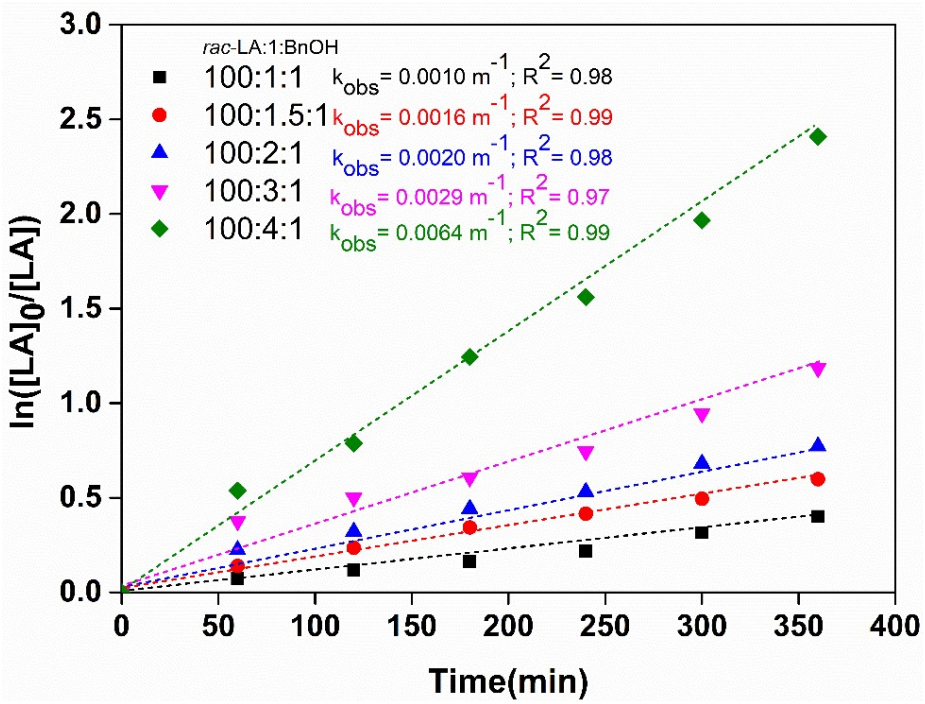

Figure FS11. First-order kinetics plots for *rac*- LA polymerizations with time in $CDCl_3$ (1 ml) with different concentrations of [κ^2-{NHI^{Dipp}P(Ph)NDipp}$MgCH_2SiMe_3$] (**1**) at 90 °C having *rac*-LA (0.072 g, 0.5 mmol)and benzyl alcohol (0.005 mmol).

Table TS8. Kinetics plots of k_{obs} vs cat [**1**] for the polymerization of *rac*-LA with [LA] = 0.5 M in $CDCl_3$ (1 ml) at 90 °C in the presence of BnOH.

S. No.	[1] (cat)	k_{obs} (m^{-1})
1	0.005	0.001
2	0.007	0.0016
3	0.01	0.002
4	0.015	0.0029
5	0.02	0.0064

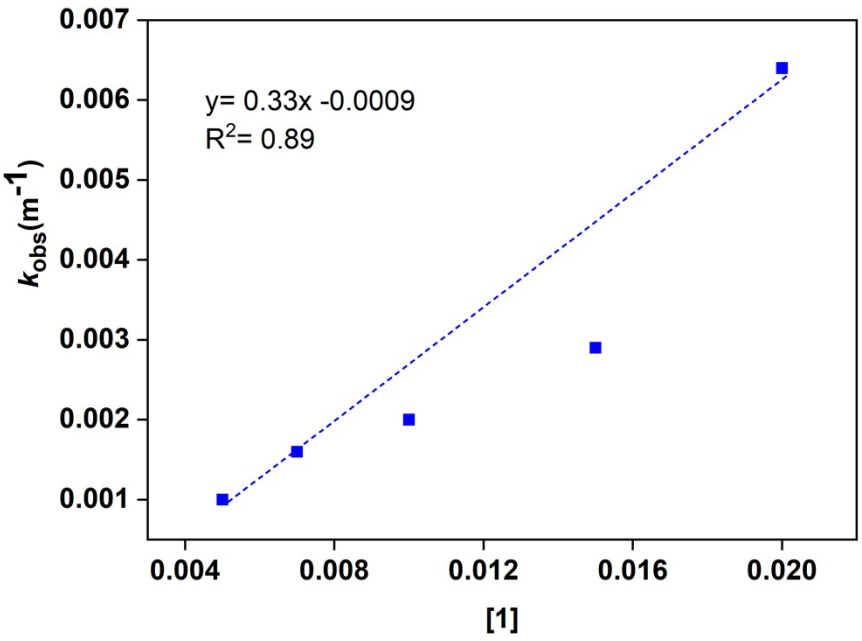

Figure FS12. Kinetics plots of k_{obs} vs [**1**] for the polymerization of *rac*-LA with [LA] = 0.5 M and benzyl alcohol (0.005 mmol) in $CDCl_3$ (1 ml) at 90 °C.

Table TS9. Kinetics plots of ln k_{obs} vs ln [**1**] for the polymerization of *rac*-LA with [LA] = 0.5 M in $CDCl_3$ (1 ml) at 90 °C in the presence of BnOH.

S. No.	ln [2]	ln k_{obs}
1	-5.29	-6.91
2	-4.96	-6.44
3	-4.61	-6.21
4	-4.19	-5.84
5	-3.91	-5.05

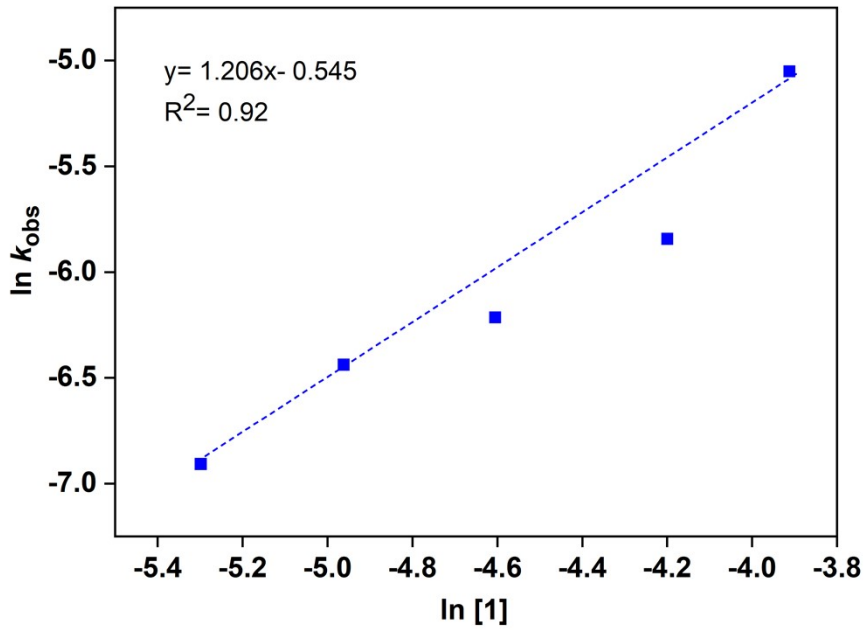

Figure FS13 Kinetics plots of ln k_{obs} vs ln [**1**] for the polymerization of *rac*-LA with [LA] = 0.02 M and benzyl alcohol (0.005 mmol) in $CDCl_3$ (1 ml) at 90 ˚C.

Further, reactions were performed by varying the concentration of BnOH (0.005, 0.01, 0.015, 0.025, 0.05 M) and keeping the catalyst **1** concentration (0.01 M) and *rac*-LA (0.072 g, 0.5 mmol) constant. The plot of $[LA]_0/[LA]$ vs. time for a wide range of **1** is linear indicating the usual first-order dependence on monomer concentration (Figure FS14) but in all cases, the value of rate constant k_{obs} remains the same. This lack of dependence on benzyl alcohol concentration confirms its zero-order contribution to the rate law (Figure FS15). Thus, the kinetics study proved that polymerization reaction does not depend on an external initiator and our catalyst itself acts as an initiator for ROP of *rac*- LA.

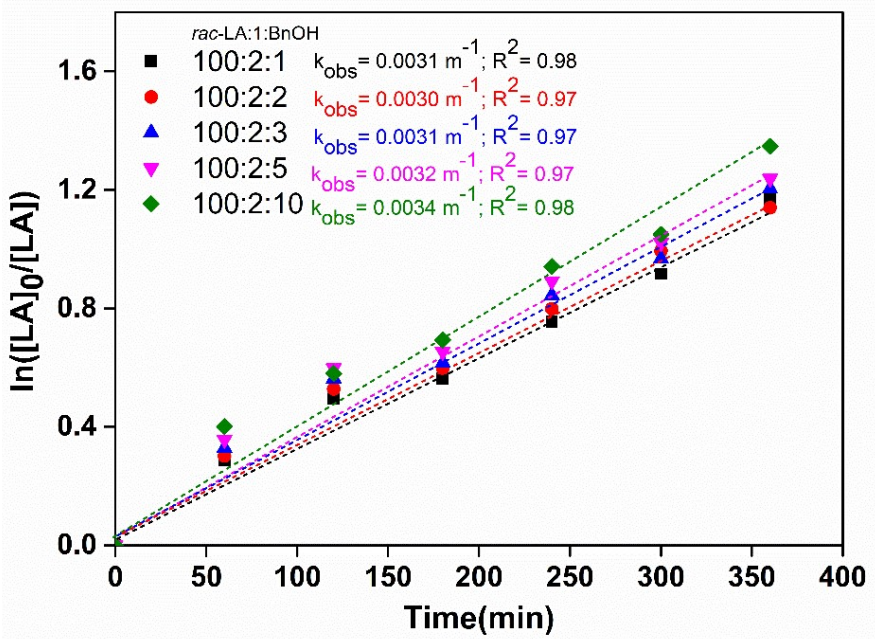

Figure FS14. First-order kinetics plots for *rac*- LA polymerizations with time in $CDCl_3$ (1 ml) with different concentrations of BnOH at 90 °C having *rac*-LA (0.072 g, 0.5 mmol) and (**1**) as catalyst (0.01 mmol).

Table TS10: Kinetics plots of ln k_{obs} vs ln (BnOH) for the polymerization of *rac*-LA with [LA] = 0.5 M in $CDCl_3$ (1 ml) at 90 °C.

S. No.	ln [BnOH]	ln k_{obs}
1	-5.29	-5.78
2	-4.61	-5.81
3	-4.19	-5.78
4	-3.69	-5.74
5	-2.99	-5.68

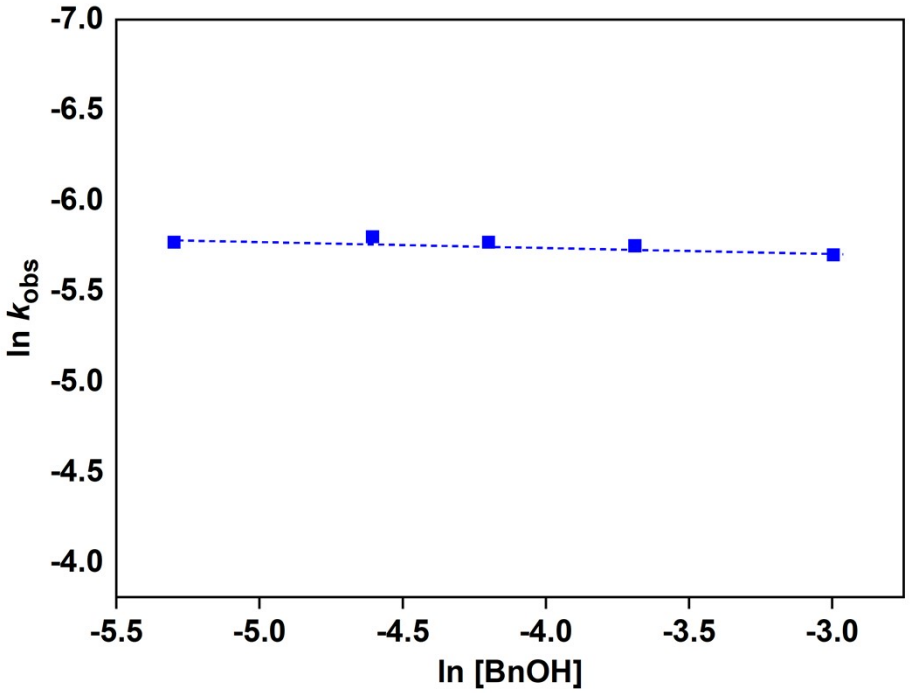

Figure FS15. Kinetics plots of ln k_{obs} vs ln [benzyl alcohol] for the polymerization of *rac*-LA (0.072 g, 0.694 mmol) and (**1**) as catalyst (0.01 mmol).

Characterization of PLA

A typical polymerization was performed at ambient temperature, *rac*-LA (0.288 g, 2.0 mmol) was added to a solution of catalyst in toluene (5 ml). After the desired reaction time, the monomer was converted into polymer, so the reaction was then quenched by the addition of a drop of 2 N HCl and methanol. Then the solution was concentrated in a vacuum, and the polymer was recrystallized with

dichloromethane and hexane. The final polymer was filtered and dried under vacuum to constant weight.

Table TS11. ROP studies of *rac*-LA using Mg catalyst **1**.[a]

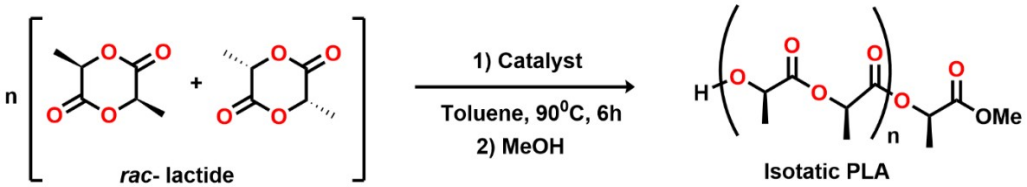

Entry	Monomer	Time (h)	Temp (˚C)	Conv[b]	$M_{n,theo}$[c] (kDa)	$M_{n,exp}$[d] (kDa)	$Đ$[d]	P_m[e]
1	100	6	90	97.1	14.0	12.7	1.2	0.85
2	200	6	90	84.0	24.2	21.1	1.3	0.79
3	300	6	90	77.5	33.5	30.6	1.2	0.75
4	400	6	90	71.4	40.0	39.7	1.5	0.73
6[f]	100	6	90	50	7.2	6.7	1.4	0.69
7[g]	100	6	90	65	9.4	7.5	1.5	0.56

[a]In toluene, [Catalyst] = 1.5 M, [b]Conversions were determined by crude mixture ^{1}H NMR spectroscopy. [c]$M_{n\,(theo)}$ = molecular weight of chain-end + 144 gmol^{-1} ×(M:1) × conversion. [d]In THF (2 mg ml^{-1}) and molecular weights were determined by GPC-LLS (flow rate ¼ 0.5 ml min^{-1}) with Mark-Houwink corrections. Universal calibration was carried out with polystyrene standards, laser light scattering detector data, and concentration detector. Each experiment is duplicated to ensure precision. [e]P_m determined by analysis of all the tetrad signals in the methine region of the homonuclear-decoupled ^{1}H NMR spectrum. [f]In THF as a solvent. [g]In presence of initiator (BnOH).

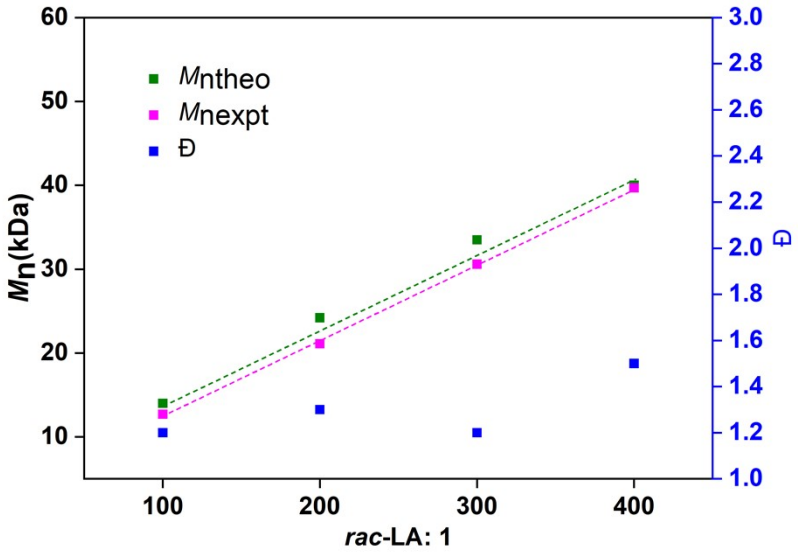

Figure FS16. A plot of theoretical, experimental M_n and molecular weight distribution of PLA as functions of the molar equivalent of *rac*-LA with respect to catalyst **1** (M_n = number average molecular weight, Dispersity ($Đ$).

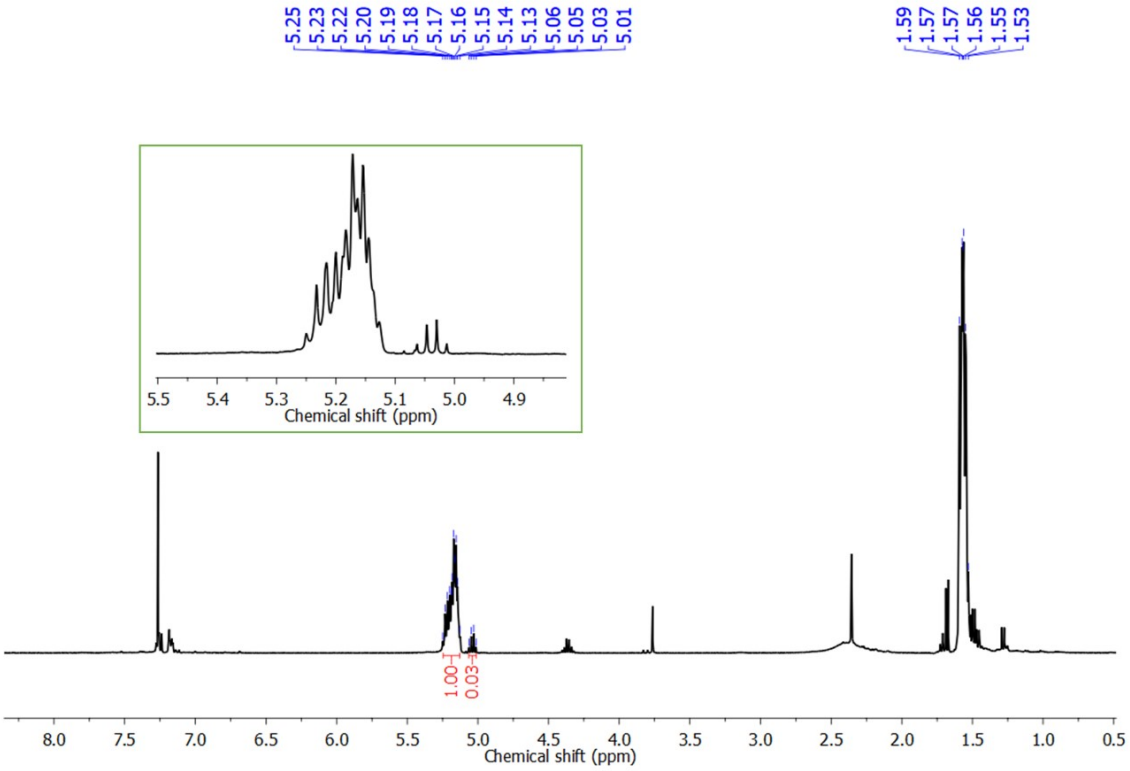

Figure FS17. ^{1}H NMR spectrum ($CDCl_3$, 25 °C) of polymerization solution sample for conversion calculation in Table TS11, Entry 1.

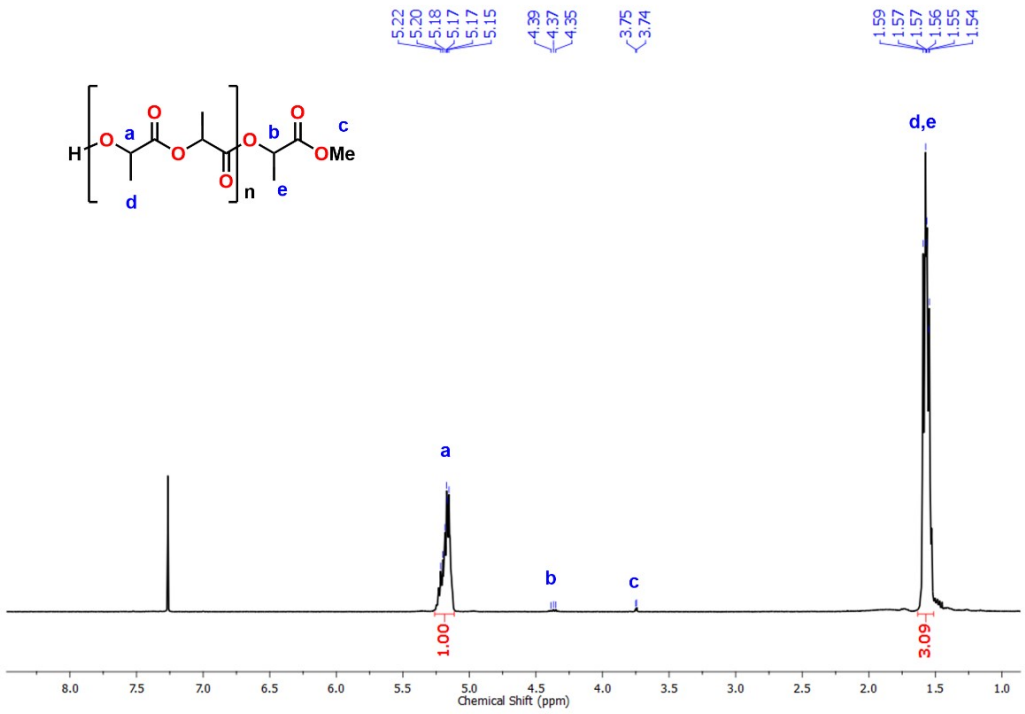

Figure FS18. [1]H-NMR spectra of PLA obtained (Entry 2 in Table TS11).

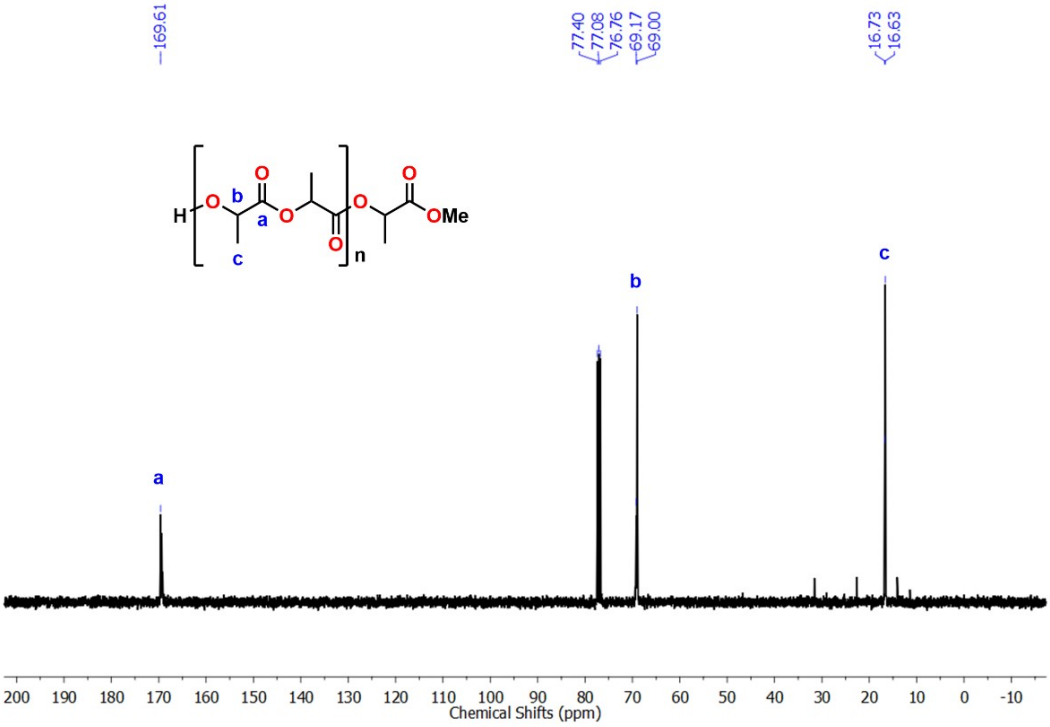

Figure FS19. [13]C-NMR spectra of PLA obtained (Entry 2 in Table TS11).

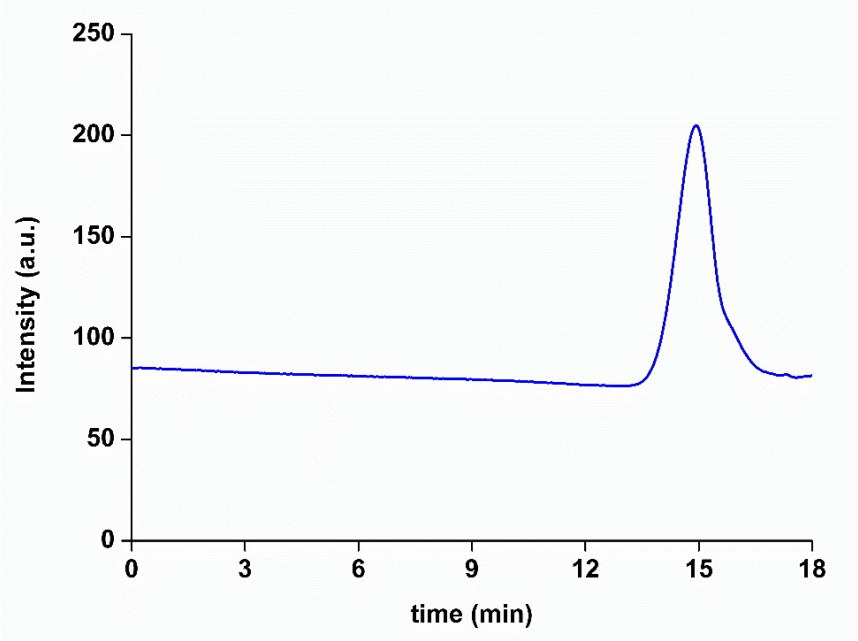

Figure FS20. GPC profile of a sample of PLA M_{nexp} = 12.7 *k*Da, PDI= 1.2 [Entry 1 in Table TS11].

Calculation of P_r / P_m Values

For ROP of lactide, there have been various well-known mechanisms such as anionic, pseudo-anionic (general base catalysis), coordination–insertion ROP and monomer-activated mechanisms. Stereocontrol polymers can be achieved via two different mechanisms, one is chain end control and the other is enantiomorphic site control. In the case of a chain end-controlled mechanism, the chirality of the propagating chain end bound to the catalyst will determine the chirality of the next monomer to be inserted which is associated with hindered catalyst systems so that the chirality of the polymer depends on the chirality of the monomer. Whereas in enantiomorphic site control, the chirality of the polymer usually depends on the chirality of the catalyst and not the chain end which determines the chirality of the next insertion. Alkali and alkaline earth metal-based catalysts are usually considered to be following stereo control in polymerization of *rac*-lactide via a chain end control mechanism and a Bernoullian statistics mode was usually employed to calculate P_m/P_r values. P_m/P_r is the probability of mesomeric /racemic linkages between monomer units determined from the methine region of the homonuclear decoupled ^{1}H NMR spectrum. P_r can also be expressed in terms of the enchainment rate constants: $P_r = k_{R/SS}/(k_{R/SS}+k_{R/RR}) = k_{S/RR}/(k_{S/RR}+k_{S/SS})$. The expressions for the tetrad concentrations in terms of P_r, assuming Bernoullian statistics and the absence of transesterification, are as follows:

Table TS12. Tetrad Probabilities Based on Bernoullian Statistics

tetrad	Probability(*rac*-lactide)
[*mmm*]	$P_m^2 + (1-P_m)P_m/2$

[*mmr*] (1-P_m)P_m/2

[*rmm*] (1-P_m)P_m/2

[*rmr*] (1-P_m)^2/2

[*rrr*] 0

[*rrm*] 0

[*mrr*] 0

[*mrm*] [(1-P_m)^2 + (1-P_m)P_m]/2

Most stereoselective ROP of *rac*-lactide in literatures involve only one single-site catalyst and the calculation of P_m / P_r usually use single-state statistic model even if in the case when *rac*-catalysts were used in ROP of *rac*-lactide.

Peak	Integration	P_m
mmm	0.75	0.82
mmr	0.04	0.91
mrm	0.07	0.88
rmm	0.03	0.93
rmr	0.04	0.73
Average		0.85

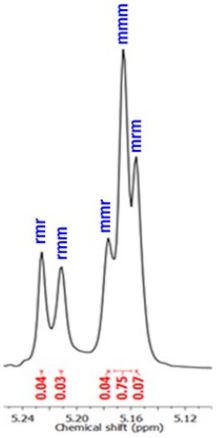

Peak	Integration	P_m
mmm	0.88	0.92
mmr	0.01	0.70
mrm	-	-
rmm	0.05	0.89
rmr	0.06	0.65
Average		0.79

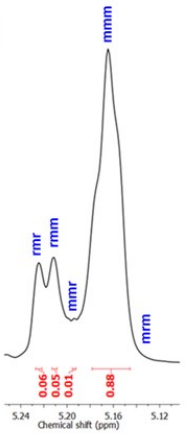

Peak	Integration	P_m
mmm	0.80	0.86
mmr	0.10	0.71
mrm	0.19	0.71
rmm	0.05	0.88
rmr	0.09	0.57
Average		0.75

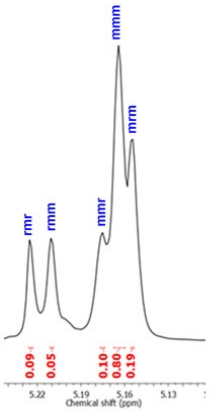

Figure FS21. $^{1}H\{^{1}H\}$ NMR spectra ($CDCl_3$, 400 MHz, 25 °C) of methine regions for PLA [Entry 1, 2 and 3, Table TS11].

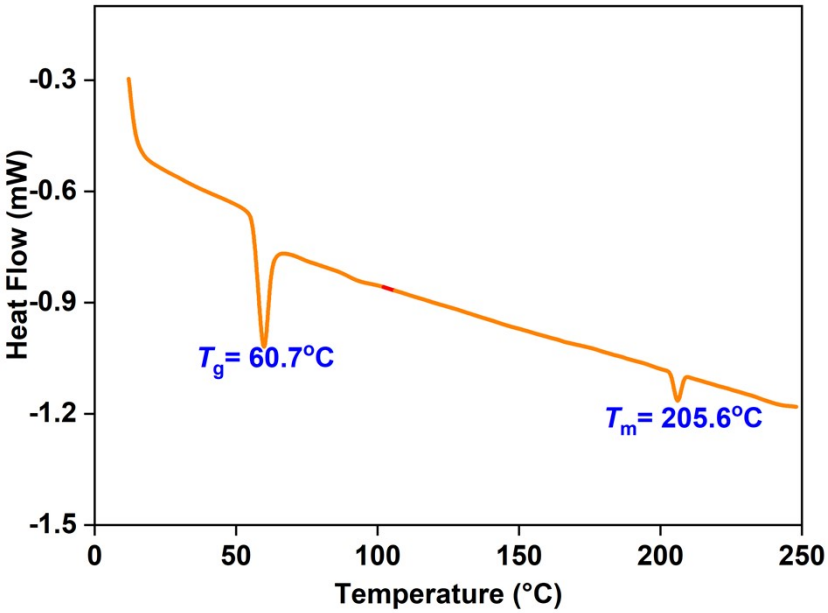

Figure FS22. DSC curve of PLA sample [Entry 1, Table TS11].

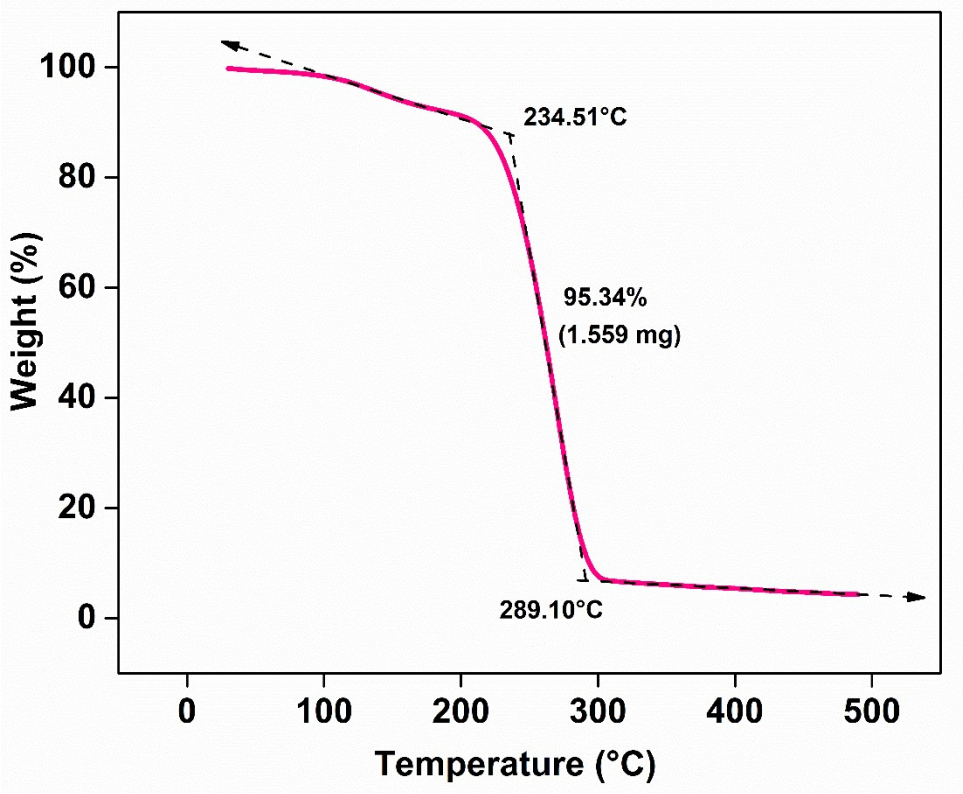

Figure FS23. TGA curve of PLA sample [Entry 1, Table TS11].

Characterisation of PCL

A typical polymerization procedure is exemplified by the synthesis of poly(ε-caprolactone) at ambient temperature (Table TS12). ε-CL (0.143 g, 1.25 mmol) was added to a solution of **1** (0.010 g, 0.0125 mmol) in toluene (4 ml). After the desired reaction time, the monomer was converted into polymer, so the reaction was then quenched by the addition of a drop of 2 N HCl and methanol. Then solution was concentrated in vacuum and polymer was recrystallized with dichloromethane and hexane. The final polymer was filtered and dried under vacuum to constant weight.

Table TS13. ROP of ε-caprolactone using Mg catalyst[a]

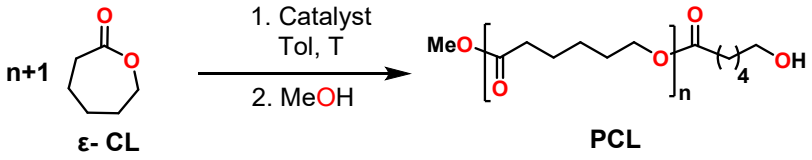

Entry	M:1	Time (min)	Temp (˚C)	Conv[b]	$M_{n,theo}$[c] (kDa)	$M_{n,exp}$[d] (kDa)	Đ[d]
1	100	30	RT	99	11.3	10.1	1.1
2	200	30	RT	99	22.6	21.6	1.2
3	300	30	RT	99	33.9	31.4	1.2
4	400	30	RT	97	44.3	42.6	1.2
5	500	30	RT	96	54.8	52.5	1.3
6[e]	100	30	60	71	8.1	-	-
7[f]	100	30	RT	77	8.8	-	-

[a]Into luene, [Catalyst] = 0.0087 mM, [b]Conversions were determined by ^{1}H NMR spectroscopy. [c]M_{ntheo}= molecular weight of chain-end + 114 gmol^{-1} ×(M:1) × conversion. [d]In THF (2 mg ml^{-1}) and molecular weights were determined by GPC-LLS (flow rate = 0.5 ml min^{-1}) with Mark-Houwink corrections. Universal calibration was carried out with polystyrene standards, laser light scattering detector data, and concentration detector. Each experiment is duplicated to ensure precision. [e]In THF as a solvent. [f]In presence of initiator (BnOH).

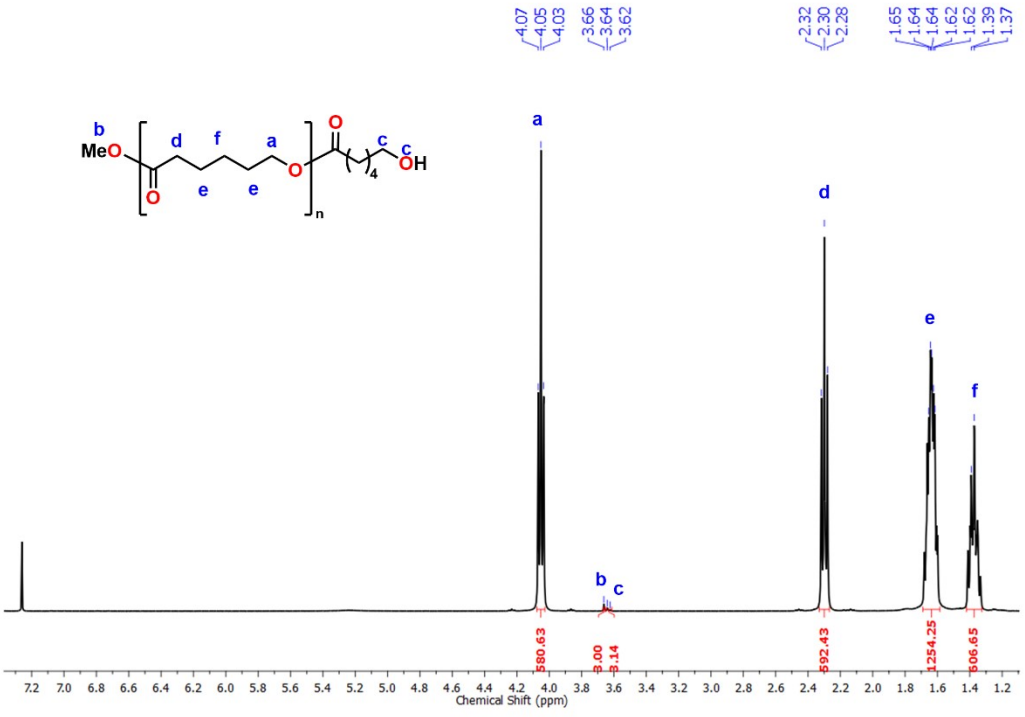

Figure FS24.^{1}HNMR spectrum (400 MHz, 25°C, $CDCl_3$) of poly(ε-caprolactone) [Entry 3, Table TS13].

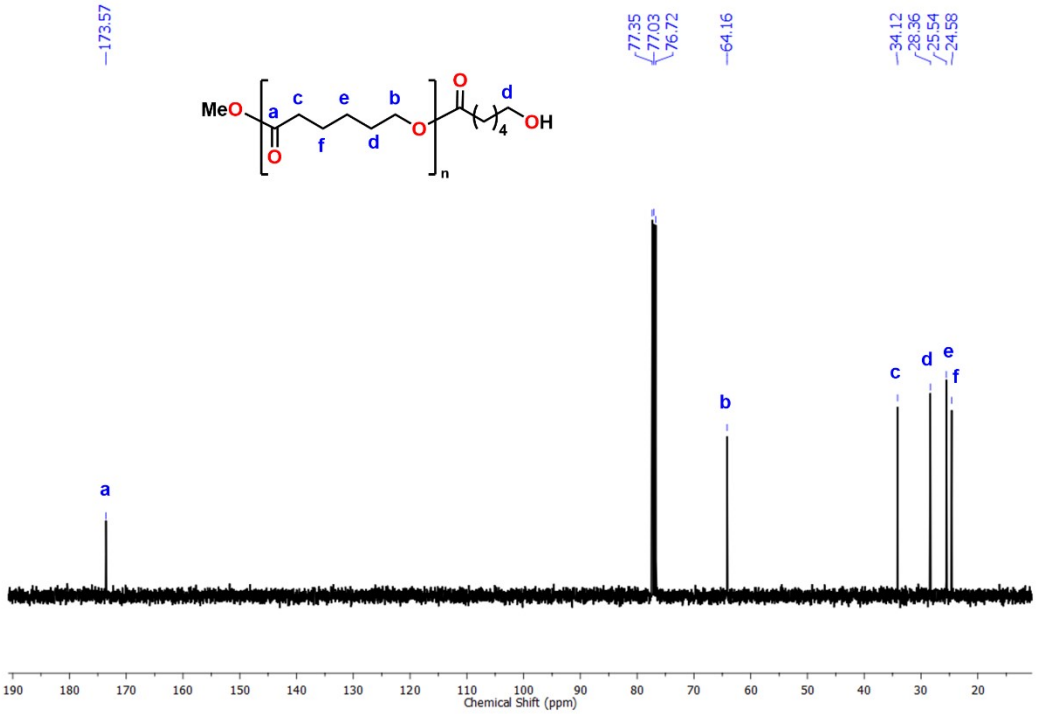

Figure FS25. ^{13}C NMR spectrum (100 MHz, 25°C, $CDCl_3$) of poly(ε-caprolactone) [Entry 3, Table TS13]

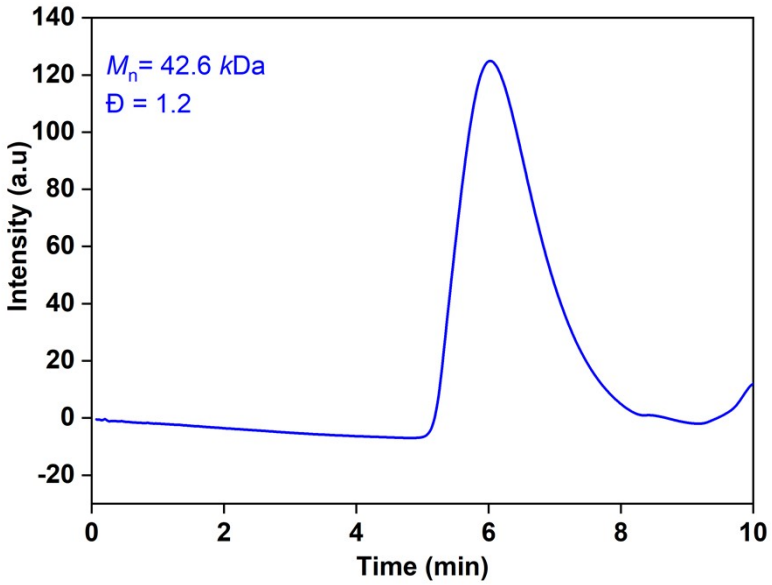

Figure FS26. GPC profile of samples of PCL [Entry 4, Table TS13].

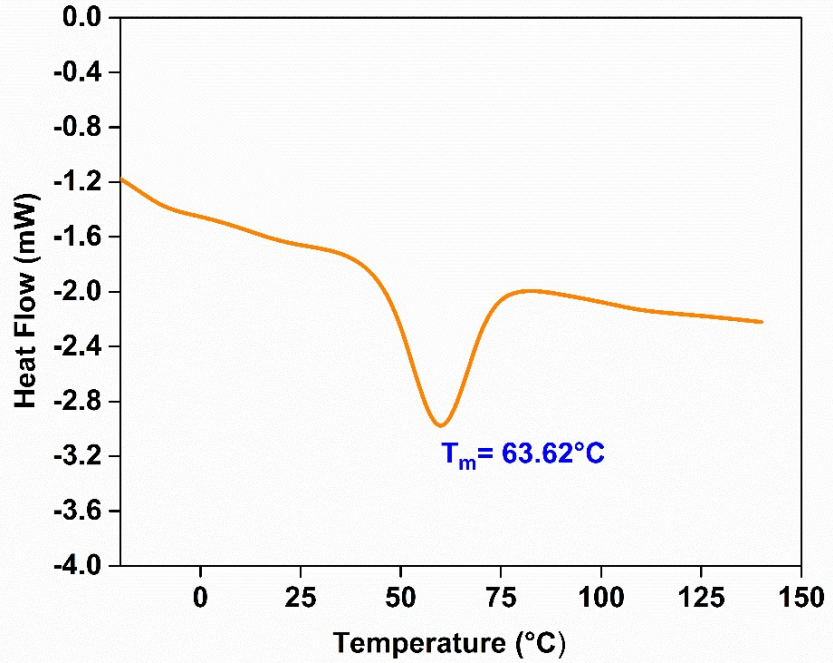

Figure FS27. DSC curves of PCL samples [Entry 3, Table TS13].

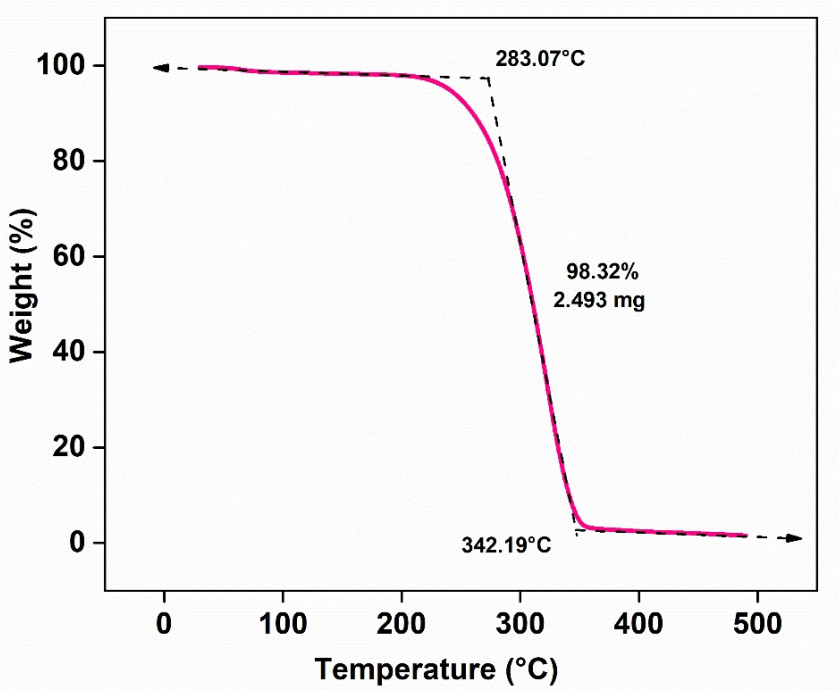

Figure FS28. TGA curves of PCL samples [Entry 3, Table TS13].

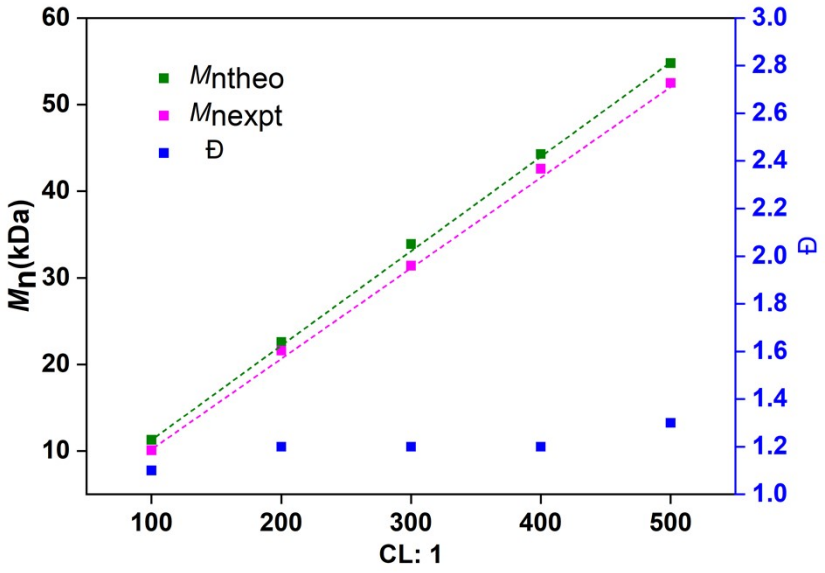

Figure FS29. Plot of theoretical, experimental M_n and molecular weight distribution of PCL as functions of ε-CL with respect to catalyst **1.**

Ring-opening copolymerization of *rac*-LA and ε-caprolactone

Procedure

For a typical copolymerization procedure was carried out via sequential addition *rac*-LA after the full conversion of CL to PCL. Initially, ε-CL (0.079 g, 0.694 mmol) was added to a solution of cat **1** (0.011 g, 0.01 mmol) in toluene (4 ml). The solution was kept at stirring at room temperature for 2h. After complete conversion of ε-CL, subsequently *rac*-LA (0.1 g, 0.694 mmol) was added. The solution was kept at stirring at 90 ^{o}C for different reaction times after which the reaction mixture was quenched by a drop of 2N HCl and methanol. Then after concentrating the solution under vacuum, the polymer was recrystallized from the mixture of dichloromethane and hexane. The final polymer was washed with methanol twice and then dried under vacuum to constant weight.

Table TS14. Block copolymerization of ε-CL and *rac*-LA and using catalyst **1**[a]

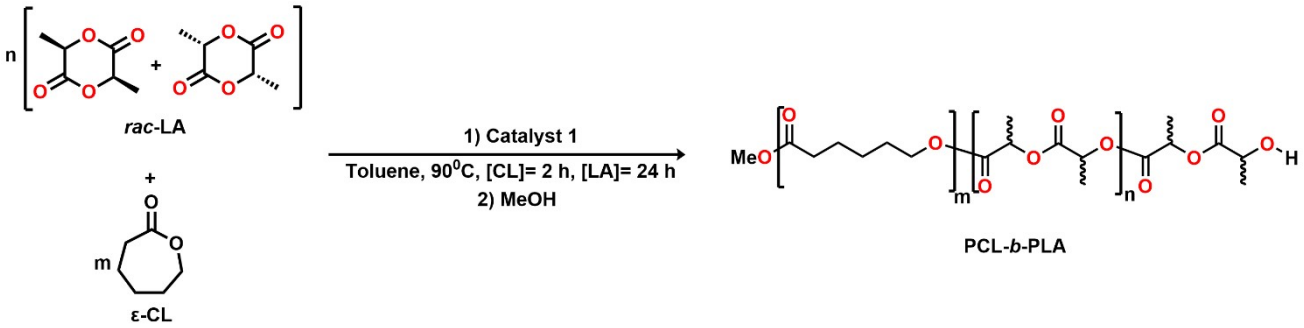

Run	[CL]: [LA]:[1]	Time (h) CL	Time (h) *rac*-LA	CL/LA[b] Conv (%)	CL/LA[c] (mol%)	Ratio of CL/LA: Terminal LA [d]	R^e	$M_{n,theo}$ (*k*Da)	$M_{n,NMR}$[f] (*k*Da)	$M_{n,exp}$[g] (*k*Da)	$Đ^g$
1	50:50:1	2	6	88.9/76.7	59.4/40.6	0.67	0.02	12.9	10.5	6.1	1.2
2	50:50:1	2	12	90.1/80.6	52.5/47.1	0.98	0.02	12.9	10.9	7.7	1.2
3	50:50:1	2	24	96.3/90.1	50.9/49.1	1	0.02	12.9	12.1	12.5	1.3
4	40:60:1	2	24	93.4/89.9	39/60.1	0.75	0.01	14.3	11.8	10.5	1.4
5	30:70:1	2	24	95.7/87.3	33/66	0.99	0.02	13.5	11.7	9.8	1.1
6	60:40:1	2	24	90.3/72.1	76.3/23.7	0.88	0.03	12.6	10.3	9.5	1.2

[a]Reaction conditions: Tol (4 ml), 90 °C. [b]Percentage conversion of the monomer determined by ^{1}H NMR spectroscopy in $CDCl_3$. [c]CL/LA mole ratio in copolymer. [d] Determined from ^{1}H NMR integrals for purified copolymer samples. [e] Randomness factor, R: R= 0 (blocky structure), R= 1 (fully random). [f]M_{nNMR} = ([CL]/[1] * %CL * 114.14) + ([LA]/[1] * % LA * 144.13). [g]Determined by GPC relative to polystyrene standards in tetrahydrofuran: M_n (GPC)= M_n (GPC) * CL (%mol in copolymer) * 0.56 + M_n (GPC) * LA (%mol in copolymer) * 0.58. Universal calibration was carried out with polystyrene standards, laser light scattering detector data, and concentration detector. Each experiment is duplicated to ensure precision.

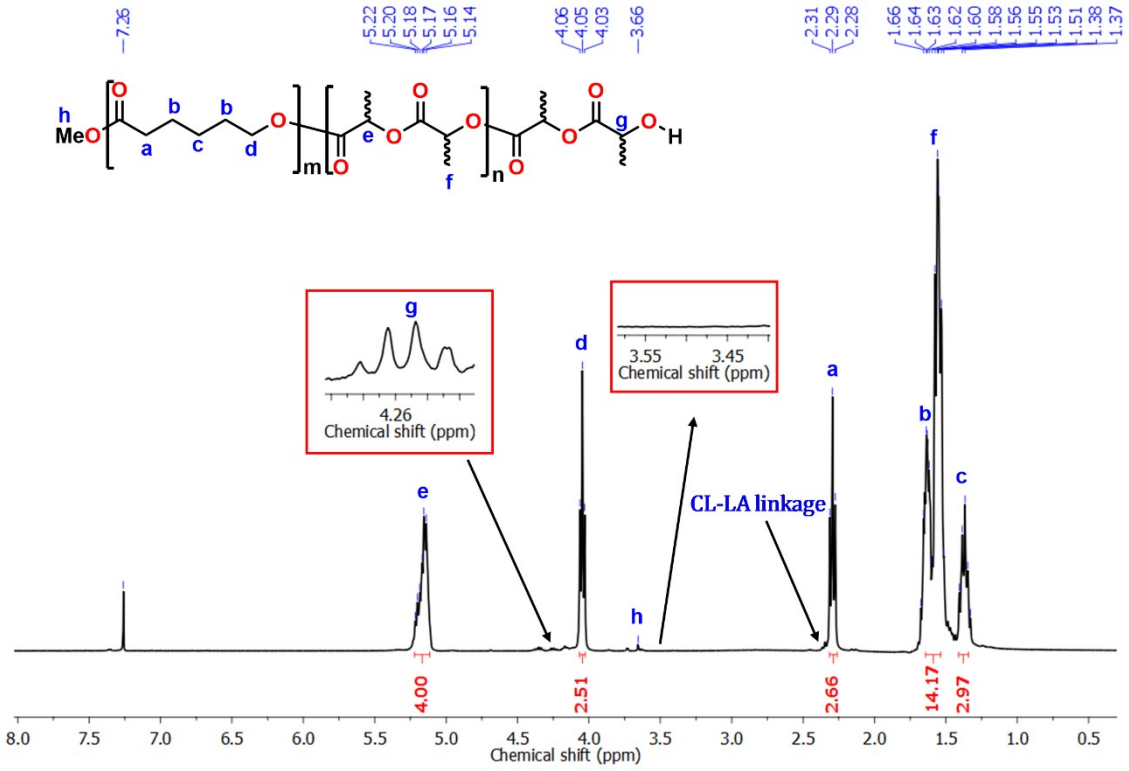

Figure FS30. [1]H NMR spectrum of a representative block copolymer (Table TS14, entry 4).

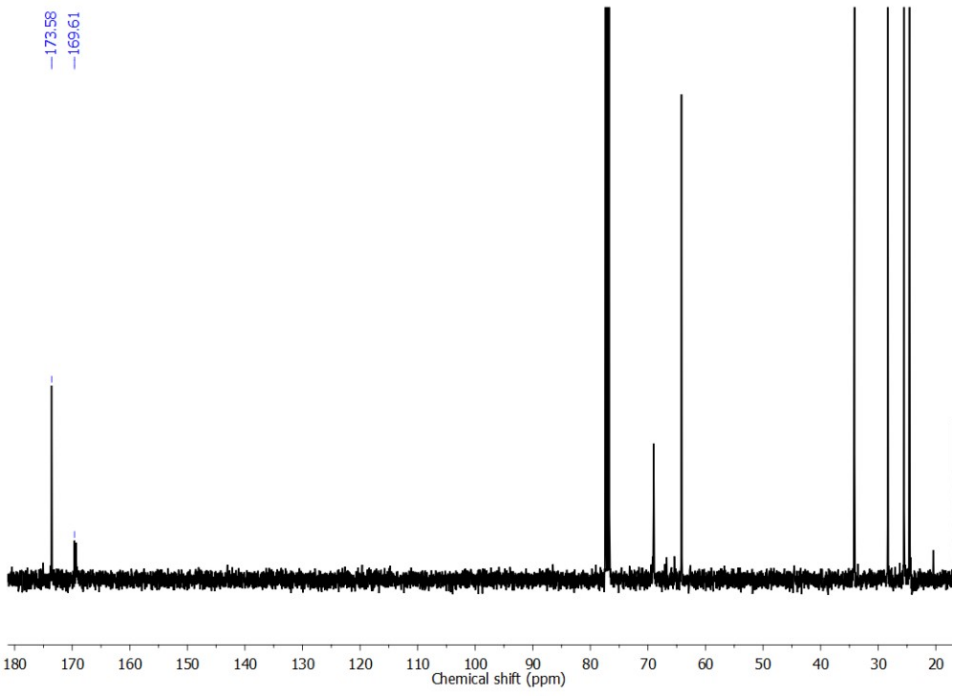

Figure FS31. [13]C NMR spectrum of a representative block copolymer (Table TS14, entry 3).

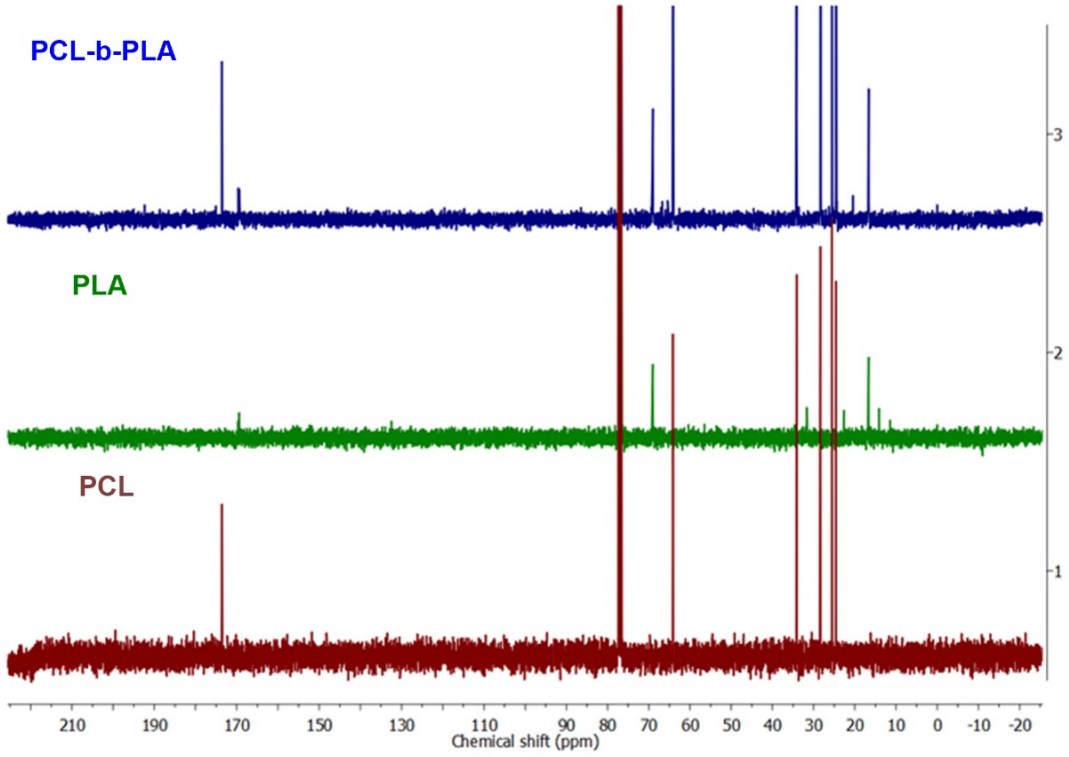

Figure FS32. Stack ^{13}C NMR spectrum of a representative di-block copolymer (Run 3), PLA, PCL.

Calculations for randomness factor, R

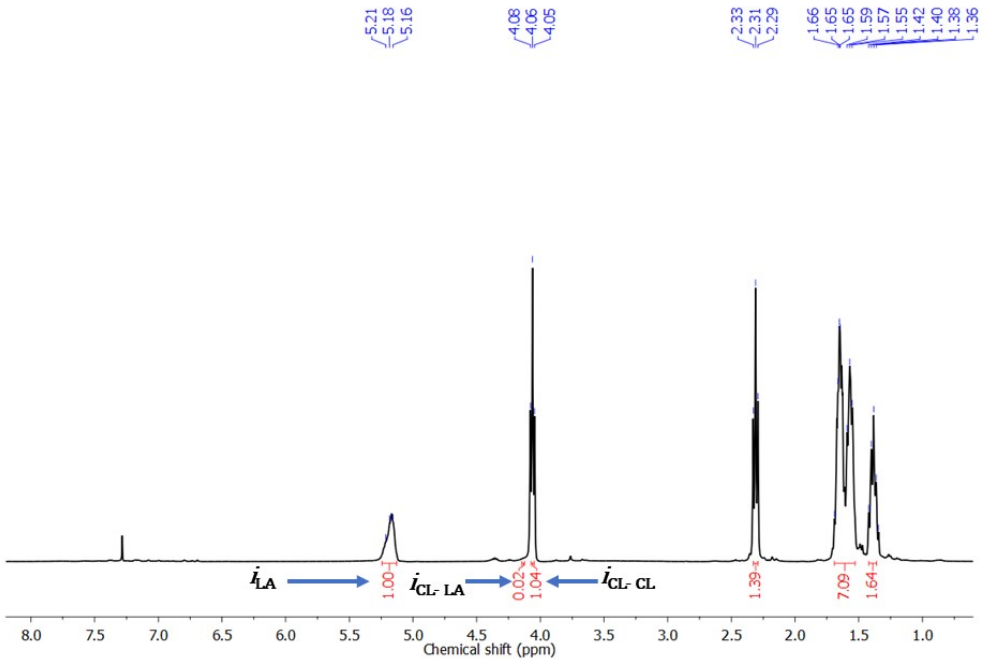

Figure FS33. ^{1}H NMR spectrum of a representative block copolymer (Table TSI4, entry 4).

The randomness factor R, were calculated using the following equations:[2]

$$i_{CL} = i_{CL\text{-}CL} + i_{CL\text{-}LA} \quad \text{and} \quad i_{LA} = i_{LA\text{-}LA} + i_{LA\text{-}CL}$$

Where f_{CL} and f_{LA} are the relative mole fraction of PCL and PLA in the copolymer, respectively

$$f_{CL} = \frac{i_{CL}}{i_{CL} + i_{LA}} \quad \text{and} \quad f_{LA} = \frac{i_{LA}}{i_{CL} + i_{LA}}$$

Following this, the average diad relative molar fractions $f_{C\text{-}C}$, $f_{C\text{-}L}$, and $f_{L\text{-}L}$, were calculated:

$$f_{C\text{-}C} = f_{CL} \times f_{C\text{-}C/CL}$$

$$f_{C\text{-}L} = f_{CL} \times f_{C\text{-}L/CL}$$

$$f_{L\text{-}L} = 1\text{-} (f_{C\text{-}C} + f_{C\text{-}L})$$

Where,

$$f_{C\text{-}C/CL} = \frac{i_{CL\text{-}CL}}{i_{CL}} \quad f_{C\text{-}L/CL} = \frac{i_{CL\text{-}LA}}{i_{CL}}$$

Randomness factor, R is calculated using the following equations:[2]

$$R = \frac{f_{C\text{-}L}}{2 \times f_{LA} \times f_{CL}}$$

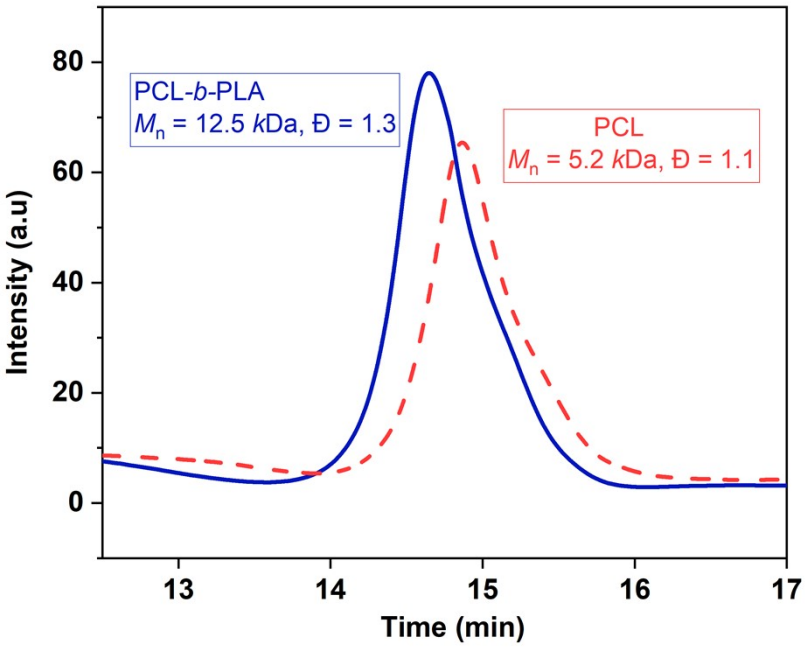

Figure FS34. GPC profile of copolymer samples [Entry 3, Table TS14].

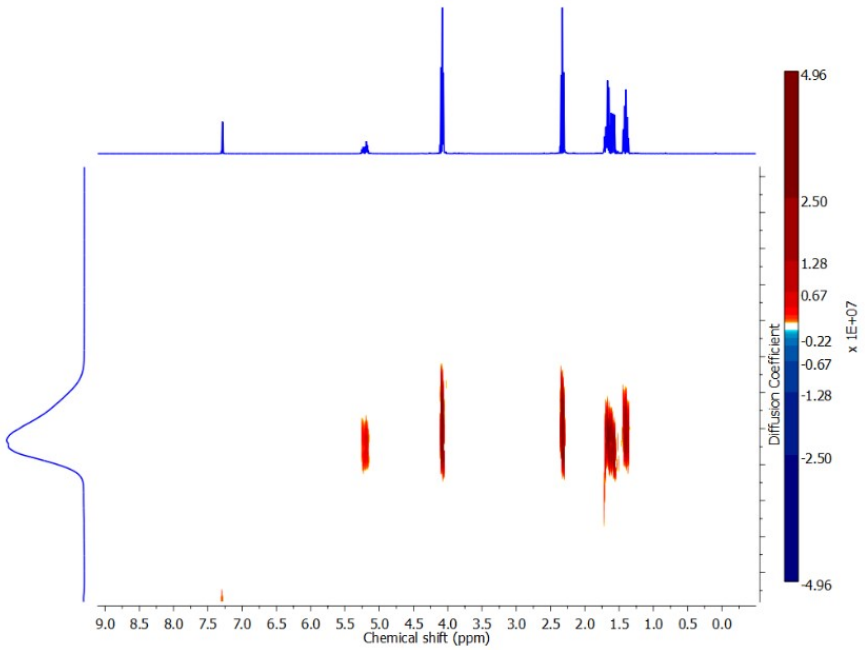

Figure FS35. DOSY NMR spectrum of the purified PCL-*b*-PLA copolymer (Table TS14, entry 3).

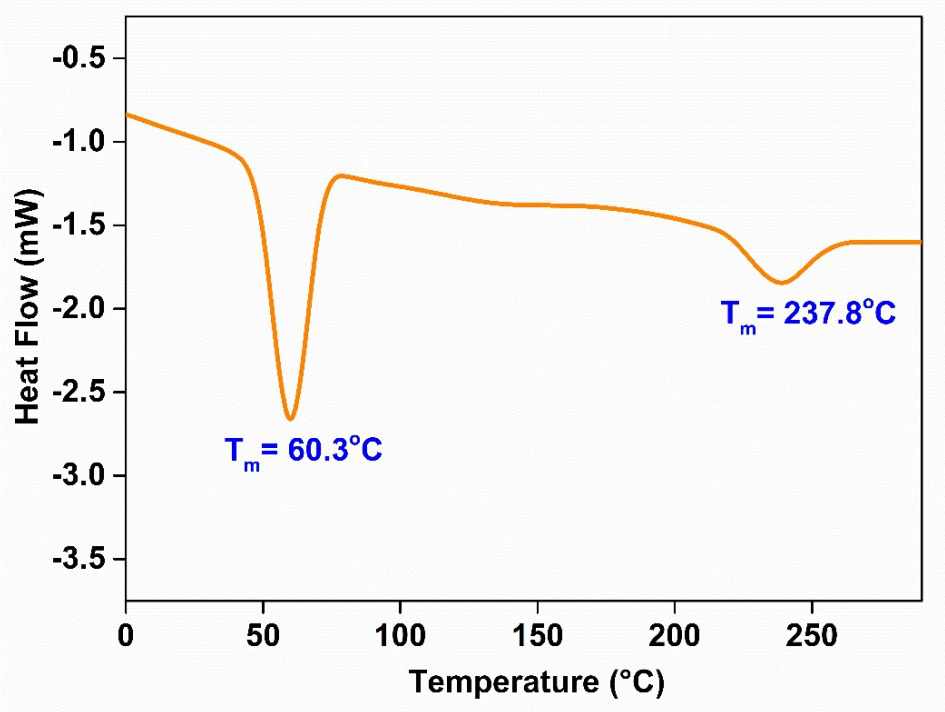

Figure FS36. DSC curve of a copolymer sample [Entry 3, Table TS14].

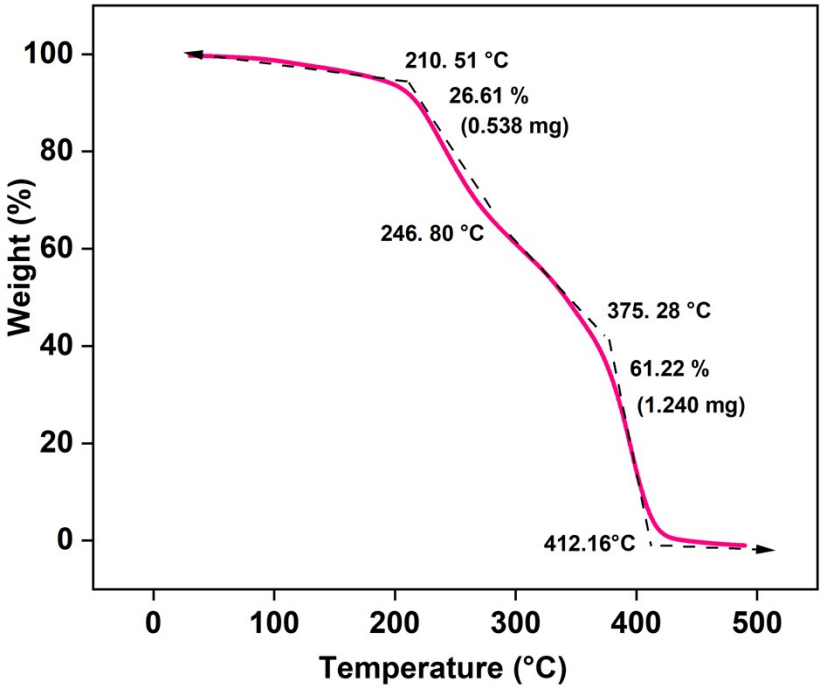

Figure FS37. TGA curve of a copolymer sample [Entry 3, Table TS14].

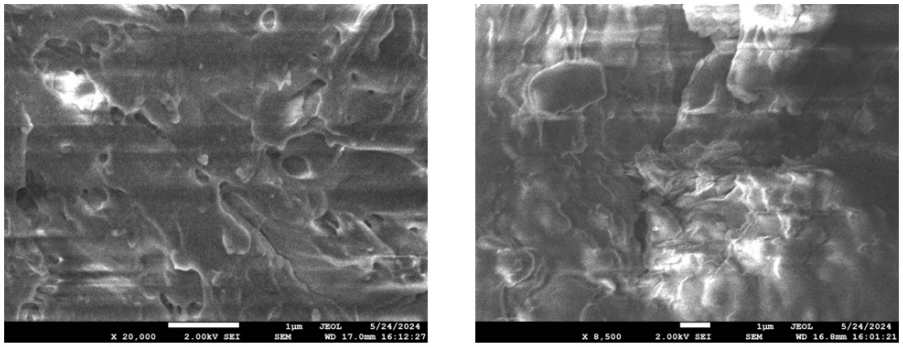

Figure FS38. Scanning electron microscopy (SEM) images of representative copolymers [Entry 3, 4 Table TS14].

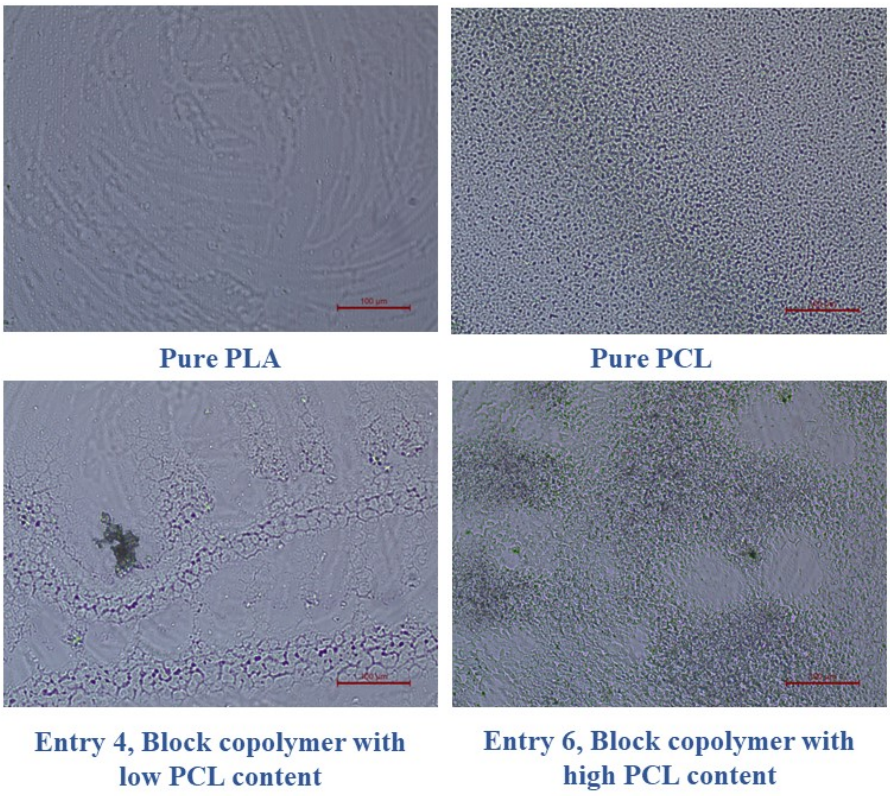

Figure FS39. Polarized Optical Micrographs pure PLA, Pure PCL, Block copolymer with low PCL content (entry 4) and Block-copolymer with high PCL content (entry 6).

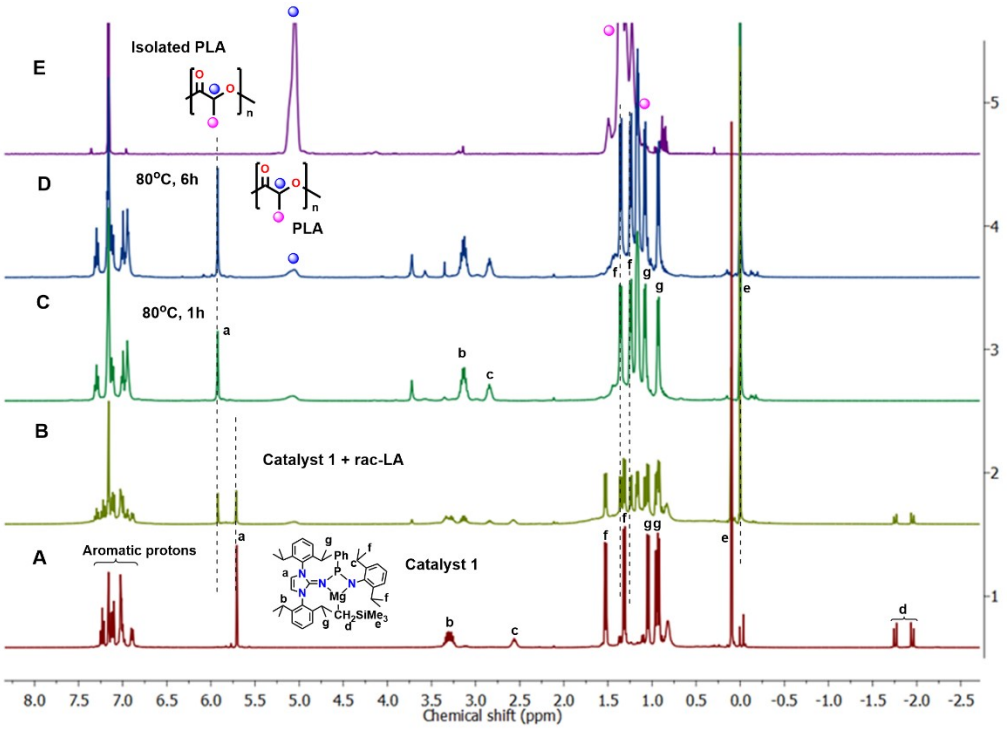

Figure FS40. Stack ^{1} HNMR spectra of the reaction between complex **1** and *rac*-LA in a 1:2 ratio in C_6D_6. (A) Complex **1** at room temperature. (B) *rac*-LA and **1** at room temperature. (C and D) *rac*-LA and **1** at 90 °C after 1 and 6 h respectively. (E) Isolated PLA

Plausible mechanism

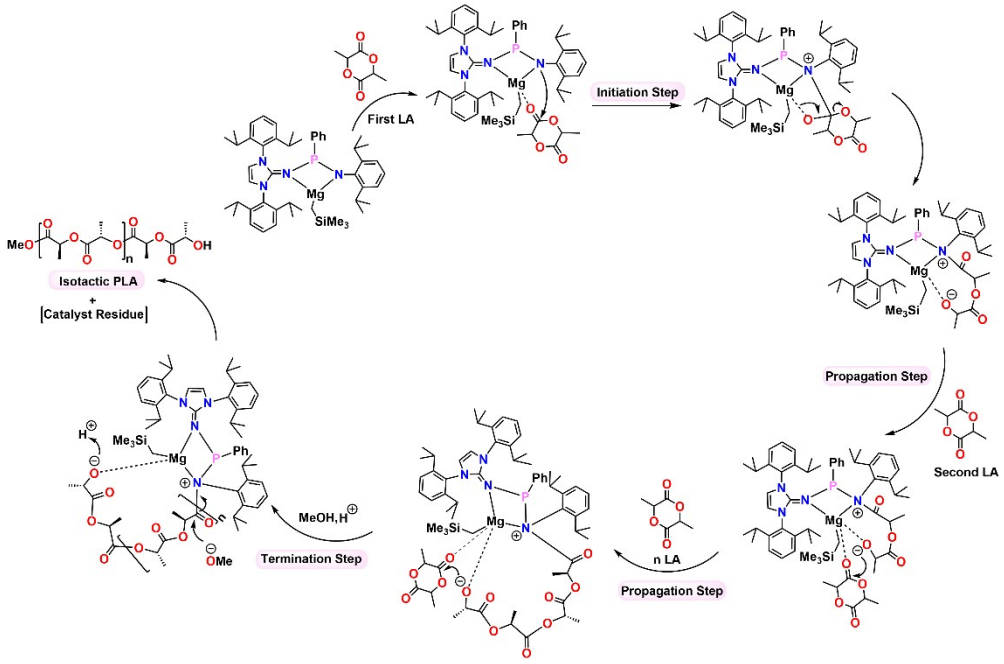

Figure FS41. ROP mechanism of *rac*-LA catalysed by catalyst **1.**

Determination of polymer tacticity

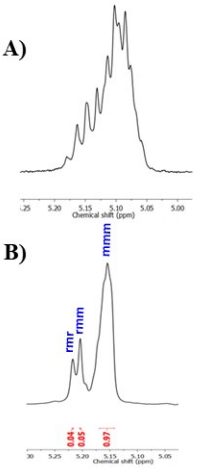

Peak	Integration	P_m
mmm	0.97	0.98
mmr	-	-
mrm	-	-
rmm	0.05	0.89
rmr	0.04	0.72
Average		0.86

Figure FS42. Example of ^1H (top) and $^1H\{^1H\}$ (bottom) NMR spectra in $CDCl_3$ used to determine tacticity of PLA backbone within the PCL-PLA block copolymer (400 MHz) [Entry 3, Table TS14][3].

End Group analysis

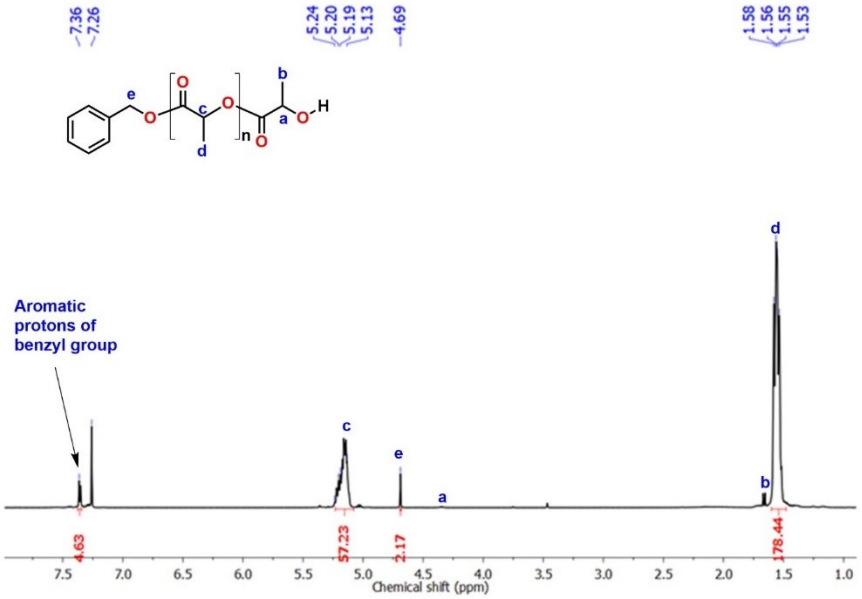

Figure FS43. ^1H NMR spectrum of PLA end capped by BnOH.

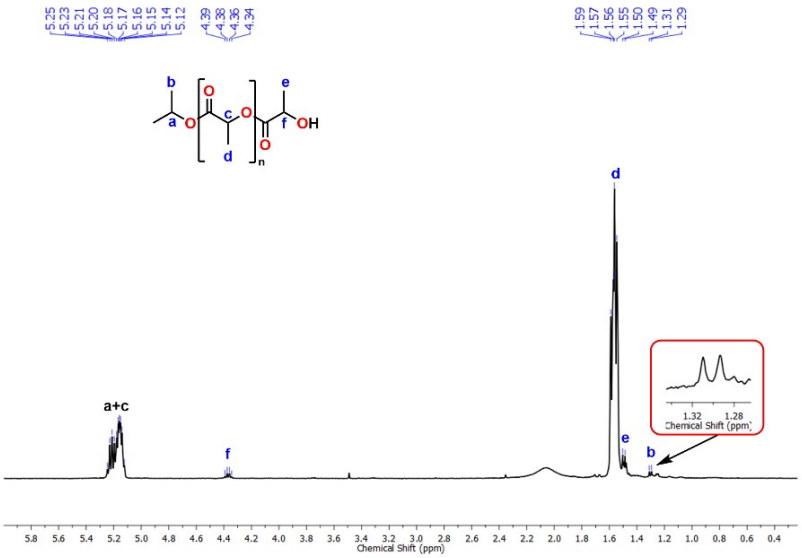

Figure FS44. ^{1}H NMR spectrum of PLA end capped by ^{i}PrOH.

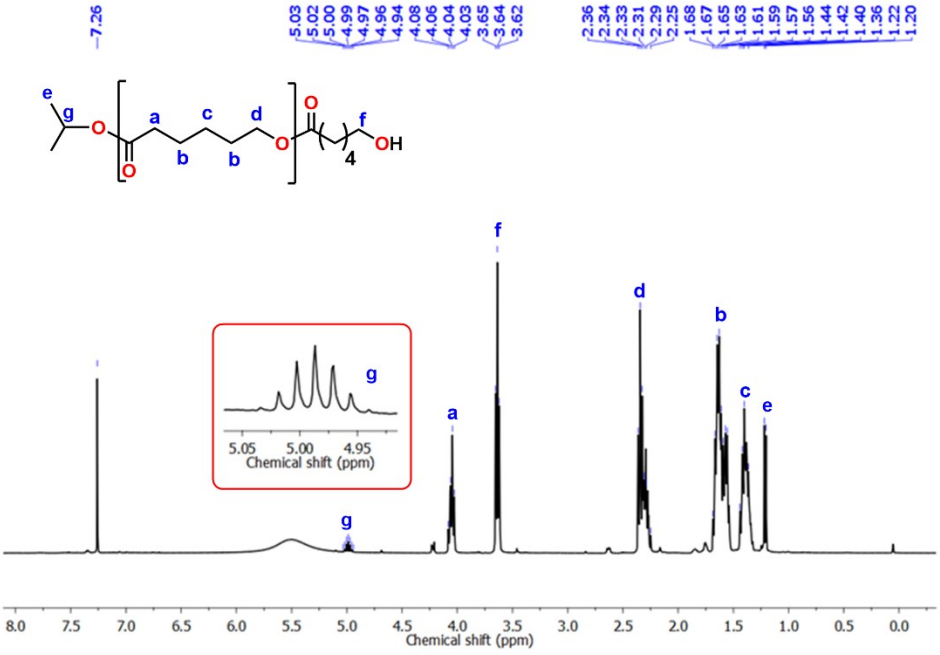

Figure FS45. ^{1}H NMR spectrum of PCL end capped by ^{i}PrOH.

References

1. H. Karmakar, S. Anga, T. K. Panda and V. Chandrasekhar, *RSC Adv*, 2022, **12**, 4501–4509.
2. J. Fernández, A. Etxeberria and J.-R. Sarasua, *J. Mech. Behav. Biomed. Mater*., 2012, **9**, 100–112.
3. T. M. Ovitt and G. W. Coates, *J. Am. Chem. Soc*., 2002, **124**, 1316–1326.